AJR FOCUS ON:

LI-RADS Categorization of Benign and Likely Benign Findings in Patients at Risk of Hepatocellular Carcinoma: A Pictorial Atlas

Reena C. Jha[1]
Donald G. Mitchell[2]
Jeffery C. Weinreb[3]
Cynthia S. Santillan[4]
Benjamin M. Yeh[5]
Ronald Francois[1]
Claude B. Sirlin[4]

OBJECTIVE. The purpose of this article is to review the imaging features and Liver Imaging Reporting and Data System (LI-RADS) categorization of benign and likely benign entities, including typical cirrhotic nodules, distinctive nodular observations, and benign entities that may simulate hepatocellular carcinoma.

CONCLUSION. LI-RADS is a system of standardized criteria for interpreting liver CT and MR images of patients at risk of hepatocellular carcinoma. Most of the observations in these patients are not malignant. With the development of fibrosis and cirrhosis, these benign entities may take on an altered appearance.

Keywords: benign liver nodules, cirrhosis, classification of liver lesions, hepatocellular carcinoma, LI-RADS

DOI:10.2214/AJR.13.12169

Received October 31, 2013; accepted after revision February 21, 2014.

R. C. Jha is a consultant for CeloNova BioSciences. J. C. Weinreb has received institutional research support from Siemens Healthcare and is a consultant for Bayer HealthCare and Siemens Healthcare. C. S. Santillan is a consultant for Robarts Clinical Research. B. M. Yeh has received a grant from and is a consultant for GE Healthcare and is a founder of Nextrast. C. B. Sirlin is a member of the advisory board and speakers bureau of Bayer HealthCare and has received a research grant from GE Healthcare.

[1]Department of Radiology, Medstar Georgetown University Hospital, 3800 Reservoir Rd, NW, Washington, DC 20007. Address correspondence to R. C. Jha (jhar@gunet.georgetown.edu).

[2]Thomas Jefferson Hospital, Philadelphia, PA.

[3]Yale School of Medicine, New Haven, CT.

[4]University of California, San Diego Medical Center, San Diego, CA.

[5]Department of Radiology and Biomedical Imaging, University of California, San Francisco, San Francisco, CA.

WEB
This is a web exclusive article.

AJR 2014; 203:W48–W69

0361–803X/14/2031–W48

The Liver Imaging Reporting and Data System (LI-RADS) is a system of standardized terminology and criteria for interpreting and reporting findings of CT and MRI examinations of the liver in patients with cirrhosis or otherwise at increased risk of hepatocellular carcinoma (HCC) [1] (Fig. 1). LI-RADS was developed by an American College of Radiology–supported committee of diagnostic radiologists with expertise in liver imaging with input from hepatobiliary surgeons, hepatologists, hepatopathologists, and interventional radiologists. It is a dynamic document that will be expanded and updated with advances in knowledge and experience. The use of LI-RADS will aid radiologists in categorizing observations seen in this at-risk population and will help referring physicians understand radiologic reports.

Cirrhosis is a risk factor for the development of HCC, and a stepwise progression of hepatocarcinogenesis has been established [2–5]. Cirrhosis is characterized by remodeling of the hepatic architecture with bridging fibrosis that alters the normal homogeneous parenchyma to various patterns of scarring and regeneration that result in a spectrum of hepatocellular nodules [2, 3]. Altered vascular dynamics also may be present and obscure or simulate malignancy. In patients at increased risk of HCC, particularly those with cirrhosis, imaging of the liver can be problematic.

LI-RADS has been developed to provide a framework for assigning degrees of concern to imaging findings. Currently, LI-RADS applies to multiphase CT and MRI performed with extracellular gadolinium-based contrast media and does not apply to hepatobiliary agents, which are actively being developed. To facilitate clarity in interpreting, reporting, and discussing imaging findings, including those of cirrhotic liver, it helps to use a carefully chosen and agreed-on vocabulary, or lexicon, that differentiates, when necessary, histologic entities (e.g., liver nodules) from imaging findings, which are referred to in LI-RADS and in this article as observations. Occasionally, an observation may be a hemodynamic phenomenon with no histologic or pathologic correlate, so it would not be appropriate to refer to it as a nodule.

LI-RADS category 1 is for observations that are definitely benign because they have features diagnostic of a benign entity or have spontaneously disappeared at a follow-up examination. LI-RADS category 2 is for probably benign observations because they have features suggestive but not diagnostic of a benign entity. LI-RADS category 3 is for observations that do not meet criteria for the other categories and therefore have a moderate probability of being either HCC or a benign entity. LI-RADS category 4 is for observations that are probably HCC but do not meet the criteria for being considered diagnostic of HCC. LI-RADS category 5 is for masses with features diagnostic of HCC because of arterial hyperenhancement in combination with lesion size, growth, and venous

phase imaging features. Observations associated with venous invasion are categorized LI-RADS 5V. After treatment, lesions previously considered LI-RADS 5 are categorized LI-RADS 5T. LI-RADS category OM (other malignancy) is used to categorize lesions that appear to be malignant but are thought to have imaging features more suggestive of malignancies other than HCC, such as cholangiocarcinoma and metastasis.

Currently available imaging-based HCC diagnostic systems (American Association for the Study of Liver Disease; European Association for the Study of Liver Disease; Asian Pacific Association for the Study of Liver Disease; Organ Procurement and Transplant Network [OPTN]) emphasize only the diagnosis of HCC [6–10]. As of October 31, 2013, in the United States the United Network for Organ Sharing assigns priority for liver transplant based on OPTN class 5, which is equivalent to LI-RADS category 5 and depends on the size and number of lesions [11].

Although these systems represent important advances, in our experience, a definite imaging diagnosis of HCC occurs in a minority of the observations depicted at CT and MRI of the liver in patients with cirrhosis or other risk factors for HCC. Hence these systems provide incomplete guidance to radiologists in the interpretation of images. LI-RADS addresses this gap by including information on the interpretation and categorization of observations other than definite HCC at various confidence levels for benign versus malignant. The differential diagnosis of such observations includes a spectrum of premalignant cirrhosis-associated nodules and benign entities that may occur in a cirrhotic liver. These premalignant nodules and benign entities are commonly encountered and may overlap in imaging appearance with HCC, causing diagnostic confusion and leading to inappropriate management.

Understanding the appearance of benign and likely benign findings in a cirrhotic liver is important for appropriate patient care. Cirrhotic nodules occur on a histologic spectrum that includes regenerative nodules, low-grade dysplastic nodules, high-grade dysplastic nodules, and HCC. The terminology of these lesions varies in the radiology literature and has evolved in the pathology literature. A detailed review is beyond the scope of this article. The textbook by Saxena [12] contains a chapter devoted to premalignant hepatocellular lesions and their terminology and clinical significance.

At imaging, benign nodules in a cirrhotic liver can be classified into three broad categories. The first is typical cirrhotic nodules, which constitute the parenchyma in a cirrhotic liver. These nodules are generally not assigned to LI-RADS categories. The second category is other benign entities that may have an altered appearance in a cirrhotic liver and may occasionally simulate HCC. Various benign entities may take on an altered appearance with the progression of cirrhosis. Benign entities frequently encountered in patients with cirrhosis or other risk factors for HCC include cysts, hemangiomas, vascular anomalies, perfusion alterations, fat deposition or sparing, confluent fibrosis, and focal fibrosis. The third category is distinctive nodulelike observations that appear different from surrounding liver parenchyma owing to their size or appearance compared with the background liver, Therefore, these observations may not be benign and may have imaging features seen in HCC or potential HCC precursor lesions (low-grade dysplastic nodules, high-grade dysplastic nodules). These are therefore assigned LI-RADS categories to communicate the radiologist's degree of concern about the likelihood of HCC.

The purpose of this article is to discuss the imaging features of benign or likely benign entities seen in patients at increased risk of HCC. Benign entities usually are categorized LI-RADS 1 (definitely benign) or LI-RADS 2 (probably benign), depending on the radiologist's level of certainty, but some benign entities with atypical or nonspecific features may be categorized LI-RADS 3 (intermediate probability of HCC) or higher.

Typical Cirrhotic Nodules

Definition

A cirrhotic liver is defined anatomically by the presence throughout the liver of fibrous septa that subdivide the parenchyma into innumerable nodules [2]. Because of their tiny size, most of these nodules are not individually discernible on conventional CT and MR images. When visible as discrete lesions at CT or MRI, typical cirrhosis-associated nodules tend to be uniform in size and other imaging features (Fig. 2).

Findings

Cirrhotic nodules are often invisible because of their size and uniform distribution throughout the liver. When discretely visible, cirrhotic nodules have the following imaging features: diameter often less than 1 cm; similar attenuation or mildly high attenuation relative to surrounding liver parenchyma on unenhanced CT images; isointense or mildly hyperintense relative to surrounding liver parenchyma on unenhanced T1-weighted MR images (Fig. 2); isointense or mildly hypointense relative to surrounding liver parenchyma on unenhanced T2-weighted MR images; and enhancing to a similar degree as surrounding liver in all phases after injection of extracellular contrast agents.

LI-RADS Categorization

Most observations with the aforementioned features are benign regenerative nodules, which simply represent expansion of the islands of hepatic parenchyma between areas of fibrosis. These nodules have benign histologic features without cellular atypia or other evidence of dysplasia or malignancy. Such nodules are expected findings in cirrhosis and require no LI-RADS categorization. Nodules larger than 2 cm or differing from background nodules are considered distinctive.

Benign Lesions and Observations That May Simulate Disease in a Cirrhotic Liver

Cysts

A cyst is a fluid-filled enclosed cavity lined by benign epithelium. Most cysts are easily recognized, cause no diagnostic confusion, and do not require reporting (Fig. 3). Radiologists may choose at their discretion to report cysts, recognizing that the confidence of diagnosis may be modality dependent. The presence of mildly atypical features or low-attenuation lesions too small to characterize at CT may require LI-RADS classification.

The two most common cysts in the liver are hepatic cysts and cystic biliary hamartomas. Peribiliary cysts are rare cysts associated with advanced cirrhosis [13, 14]. In cirrhosis, they represent cystic dilatation of the extramural glands in the periductal connective tissue. They parallel the bile ducts and therefore may be misinterpreted as dilated bile ducts. Hepatic cysts, cystic biliary hamartomas, and peribiliary cysts do not communicate with the bile ducts.

Peribiliary Cysts

Definition—Peribiliary cysts are cystic structures that parallel the bile ducts. They are associated with advanced cirrhosis. These cysts do not communicate with the bile ducts, and peripheral bile ducts are not dilated.

Findings—The recognition of peribiliary cysts as benign cystic structures is usually straightforward, although they may be misinterpreted as focal dilatations of bile ducts rather than cysts that parallel but do not communicate with ducts (Fig. 4).

LI-RADS categorization of cysts and peribiliary cysts—Typical hepatic cysts should be categorized LI-RADS 1, and radiologists at their discretion may choose to report these lesions. Peribiliary cysts may or may not be reported at the discretion of the interpreting radiologist. If reported, they should be assigned LI-RADS 1, because they do not resemble HCC. Observations that are indeterminate for cysts versus HCC should be categorized LI-RADS 2, 3, or 4.

Hemangiomas

Definition—Hemangiomas are a common benign tumor consisting of vascular channels lined with endothelial cells.

Findings—Hemangiomas are seen less frequently in cirrhotic than in normal liver. Hemangiomas in patients with mild or early cirrhosis may have typical imaging features and therefore can be diagnosed as hemangiomas on the basis of those features (Fig. 3), which are as follows: peripheral discontinuous nodulelike expanding enhancement or rapid enhancement (flash-filling) and signal intensity of enhancing portion that parallels blood pool enhancement; sharply circumscribed border; round, oval, or lobulate shape; low attenuation on unenhanced CT images; low T1 signal intensity on unenhanced MR images; markedly high T2 signal intensity; and high signal intensity on diffusion-weighted MR images (due at least in part to T2 shine-through).

With progression of fibrosis, a hemangioma may become smaller and occasionally fill in with fibrosis (sclerosed or hyalinized hemangioma) and acquire atypical features (Figs. 5–7) potentially leading to diagnostic confusion and incorrect interpretation [14–16].

Atypical features may include the following: atypical morphologic features, including less distinct margins and lower signal intensity on T2-weighted images; involution and size reduction over time; rimlike enhancement in arterial phase; incomplete filling-in on late phase images; and disappearance of the hemangioma.

LI-RADS categorization—Images from previous examinations can be helpful for finding changes of involution. If no previous images are available, a hemangioma with an atypical enhancement pattern may be categorized LI-RADS 2, 3, or 4 and require close follow-up. It is important that a hemangioma with an atypical enhancement pattern not be categorized LI-RADS 5.

Vascular Anomalies

Definition—Vascular anomalies are abnormal communication between hepatic vascular systems.

Findings—Vascular anomalies are focal masslike observations that often exhibit arterial phase enhancement with early enhancement of the adjacent portal vein or hepatic vein. Arterioportal and portohepatic venous fistulas are common examples. The patient may have a history of percutaneous liver biopsy (Fig. 8) or transjugular liver intervention [17, 18]. In patients with cirrhosis, spontaneous intrahepatic varices may simulate a mass, but the enhancement pattern parallels the portal venous system. Occasionally, vascular anomalies may be congenital or occur in syndromes, such as Osler-Weber-Rendu syndrome, characterized by multiple intrahepatic vascular malformations [19, 20].

LI-RADS categorization—Vascular anomalies are categorized LI-RADS 1, 2, or 3 depending on the imaging features.

Perfusion Alterations or Transient Hepatic Intensity, Attenuation, and Enhancement Differences

Definition—Transient hepatic intensity and attenuation differences (THIDs and THADs) and enhancement differences are geographic, often well-defined regions of perfusion alteration characterized by transient arterial phase hyperenhancement relative to background liver [21–25] (Figs. 9 and 10). Causes include the following: arterioportal shunting due to cirrhosis (Fig. 9), biliary ductal dilatation, tumor (benign or malignant), arterioportal fistula from previous biopsy (Fig. 8), or other trauma and obstruction of a portal vein branch with a compensatory increase in arterial flow to the region supplied by the portal vein branch (Fig. 10). Portal branch obstruction may be due to thrombosis (benign or malignant) or external compression (benign or malignant) that results in compensatory increased arterial flow caused by the hepatic arterial buffer system [26, 27].

Findings—THIDs and THADs are characterized by arterial phase hyperenhancement followed by delayed phase isointensity or isoattenuation relative to background liver (Fig. 9). They are invisible on unenhanced images but may have abnormal signal intensity on these images when associated with malignancy. Three morphologic patterns may be observed: geographic or peripheral wedge-shaped regions of increased enhancement in the arterial phase compared with background liver parenchyma; nodular, referred as nodulelike arterial phase hyperenhancement; and florid and patchy, possibly mimicking infiltrative or multifocal HCC. Key imaging features that usually help differentiate THID and THAD from HCC include the following: visible only on arterial phases; invisible on unenhanced images and on images from the later phases of contrast enhancement (Figs. 8–10); and not masslike.

LI-RADS categorization—Wedge-shaped THIDs and THADs can usually be assigned to LI-RADS category 2. Nodular or florid THIDs and THADs can be classified as LI-RADS 3 or, conceivably, LI-RADS 4. It is important that THIDs and THADs, even if nodular or florid, not be falsely assigned to LI-RADS category 5. Although THIDs and THADs are benign, HCC nodules obstructing or invading portal vein branches may cause them. If present, such nodules are usually located at the apex of the THID or THAD. Because the apex of the THID or THAD can contain an HCC nodule, the apex of wedge-shaped THIDs and THADs should be scrutinized for focal LI-RADS observations, and the observations should be scored according to LI-RADS criteria.

Hepatic Fat Deposition or Sparing

Definition—Hepatic fat deposition or sparing is the presence of excess lipid within hepatic parenchyma. Hepatic fat deposition can be diffuse, focal, or multifocal [28–33]. It should be differentiated from intralesional fat (see later, Steatotic Nodules).

Findings—MRI is more sensitive and specific than CT for the detection of hepatic fat deposition. At MRI, hepatic fat deposition may be diagnosed if the liver, in whole or in part, exhibits loss of signal intensity on T1-weighted out-of-phase compared with T1-weighted in-phase gradient-echo images or on fat-suppressed compared with non–fat-suppressed images (Figs. 11–15). At CT, hepatic fat deposition may be diagnosed if the attenuation of the liver, in whole or in part, measures 40 HU or less on unenhanced or enhanced images or 10 HU or more lower than the attenuation of the spleen on unenhanced images (Fig. 11).

Fatty infiltration has no mass effect, and vessels course through the region without

displacement. Furthermore, because fatty infiltration is composed of normal hepatocytes, the area of fatty infiltration has enhancement that parallels the unaffected liver in all phases of scanning. This may appear as if an area of lower signal intensity or attenuation were stamped on the liver. Diffuse hepatic fat deposition affects a large area of the liver (entire liver, lobe, or segment) and may have a homogeneous distribution or a heterogeneous distribution that is patchy, perivascular, subcapsular, or multisegmental (Figs. 12–15). Focal hepatic fat deposition affects a small area of the liver (subsegmental), usually has a geographic shape, and is often subcapsular. Less commonly it has a rounded shape (Figs. 13 and 14). It usually occurs in specific areas (e.g., adjacent to the porta hepatis, gallbladder fossa, falciform ligament, and ligamentum venosum). Hepatic fat deposition may overlap in imaging appearance with solitary or multiple expansile masses or with infiltrative masses (Fig. 15).

Hepatic Fat Sparing

Definition—Hepatic fat sparing is lack of lipid or relative lack of lipid within a portion of otherwise fatty hepatic parenchyma [28, 29].

Findings—MRI is more sensitive and specific than CT in the detection of hepatic fat sparing. At MRI, hepatic fat sparing may be diagnosed if the liver shows area of less loss of signal intensity on T1-weighted out-of-phase compared with T1-weighted in-phase gradient-echo images or on fat-suppressed compared with non–fat-suppressed images (i.e., liver is fatty). At CT, hepatic fat sparing may be diagnosed if the attenuation of the liver is fatty and one or more portions of the liver are hyperattenuating relative to the rest of the fatty liver.

Fat sparing is usually focal and occurs in similar areas as focal hepatic fat deposition (e.g., adjacent to the porta hepatis, gallbladder fossa, liver capsule [Fig. 11], falciform ligament, and ligamentum venosum). In a diffusely fatty liver, it may occur around the margin of a mass or in an area with impaired portal venous perfusion, likely because this vascular alteration results in less delivery of fat to the affected hepatocytes. Focal hepatic fat sparing may overlap in imaging appearance with expansile masses (solitary or multiple). Multiplanar images may help correctly characterize observations as hepatic fat sparing by showing undistorted vessels traversing the spared areas, geographic shape, and absence of mass effect.

LI-RADS categorization—Observations thought to definitely represent hepatic fat deposition or sparing should be categorized LI-RADS 1. Observations thought to probably represent hepatic fat sparing or deposition should be categorized LI-RADS 2. Observations that are indeterminate for hepatic fat deposition or sparing versus HCC may be categorized LI-RADS 3 or 4, depending on additional features.

Focal Scars and Confluent Fibrosis

Definition—Focal fibrosis and confluent fibrosis occur in regions of severe hepatic parenchymal damage and hepatocellular destruction. Confluent fibrosis is more common in primary sclerosing cholangitis, secondary biliary cirrhosis, and alcoholic liver disease than in viral liver disease.

Findings—The findings of focal fibrosis and confluent fibrosis are sheetlike, bandlike, or wedge-shaped areas, often subcapsular, of abnormal signal intensity or attenuation [34–37] that often progress over time. Classic findings are increased signal intensity on T2-weighted MR images and decreased signal intensity on T1-weighted images (Figs. 16 and 17). On unenhanced CT images, scars or fibrosis generally have decreased attenuation. They have straight borders and are concave. They may exhibit associated retraction of the liver capsule. Contrast-enhanced images generally show enhancement that is progressive and peaks in the delayed phase after extracellular contrast administration.

The CT attenuation, MRI signal intensity, and enhancement characteristics of scars and fibrosis can overlap those of cholangiocarcinoma and HCC. Unlike the geographic appearance of fibrosis, the appearance of hepatic tumors is masslike and rounded (Fig. 18). Intrahepatic nodular cholangiocarcinoma may exhibit focal retraction of the liver capsule [38, 39]. The enhancement pattern of this malignancy is often peripheral or targetlike and heterogeneous on early phase images. Progressive delayed enhancement occurs.

A change in a focal area of presumed fibrosis into a more masslike appearance or the occurrence of progressive lobar atrophy out of proportion to the fibrosis and scarring in the rest of the liver should raise concern about cholangiocarcinoma, particularly in patients with risk factors for this tumor.

LI-RADS categorization—Confluent fibrosis and focal scars usually are assigned to LI-RADS category 2, 3, or occasionally 4, depending on other features. The presence of characteristic morphologic features and location usually leads to correct interpretation and appropriate categorization as LI-RADS 1 or 2, depending on level of confidence.

Observation That Spontaneously Disappears at Follow-Up

Definition—An observation may have been previously classified and reported as LI-RADS category 2 or greater but owing to variability in image quality and phase of enhancement may no longer be seen.

Findings—Certain typical or atypical nodules may no longer be seen owing to differences in the degree of hepatic steatosis or iron deposition over time. In addition, focal lesions such as hemangiomas may disappear as part of evolutionary changes of advancing cirrhosis. Nodulelike arterial phase hyperenhancement and perfusion abnormalities can also change owing to changes in vascular milieu and overall hepatic perfusion [24, 40, 41].

LI-RADS categorization—Lesions may be reclassified on the basis of interval changes after careful analysis for changes in technique that may explain the disappearance or poor visualization of the lesion.

LI-RADS reporting—Downgrading of a lesion should be reported. Radiologists should discuss with the patient's hepatologist the potential downgrading of lesions that have previously been categorized LI-RADS 4 or 5 in patients considered for liver transplant, because this may complicate their treatment. If technical reasons do not allow classification of a previously described lesion classified LI-RADS 3 or higher, this should be stated.

Distinctive Nodulelike Observations

Definition

Nodular observations in a cirrhotic liver that do not have the imaging features described earlier and are atypical compared with the rest of the background liver may be considered distinctive. Nodules distinctly different from background nodules usually require LI-RADS categorization because there is greater likelihood that the nodules represent low-grade dysplastic nodules, high-grade dysplastic nodules, or HCC.

Hepatocarcinogenesis is believed to occur in a stepwise manner from dysplastic change to HCC [4, 5]. The observation that a nodule stands out from the overall appearance of the innumerable background cirrhotic nodules should alert the radiologist to analyze the features of this observation in all MRI sequences and all phases of contrast enhancement at CT

and MRI. A search must be made for changes in size, morphologic features, attenuation and signal intensity, and enhancement features compared with previous images, and whether ancillary features of malignancy are present must be determined. At times, it may not be possible to confidently determine whether the nodule is benign or malignant. Distinctive nodules may correspond to various pathologic entities, such as regenerative nodules, dysplastic nodules, and HCC. The most critical distinction is between HCC and non-HCC, although the possibility of another malignancy, such as cholangiocarcinoma, must be kept in mind. Occasionally, no pathologic findings correspond to the nodular observation.

Findings

Nodules that do not meet the criteria for typical cirrhotic nodules are seen as distinctive nodular observations. These include large (≥ 2 cm) nodules distinct from the rest of the liver; nodules with unenhanced signal intensity or attenuation different from that of background liver (the distinctive unenhanced signal intensity or attenuation may be due to the presence of copper, hemorrhage, fat, glycogen, or iron); nodules that enhance differently from surrounding liver, undergoing either focal or diffuse arterial phase hyperenhancement or delayed phase hypoenhancement (without both patterns, because these would be suspicious for HCC); and nodules that grow over time. Threshold growth (diameter increase > 50% within 6 months and 100% over 12 months) is a major feature of HCC [1].

LI-RADS Categorization

Nodular observations that at imaging are truly distinct from background nodules because of higher fat content, iron content, or T1 signal intensity may be dysplastic and hence merit categorization as LI-RADS 2 or greater. For this reason, these distinctive nodules usually warrant inclusion as observations in LI-RADS reports and extra attention at current and follow-up studies. If the nodule has one feature that is atypical, other features must be analyzed to best assign a LI-RADS category. For example, if a lesion is larger than 2 cm but has high signal intensity on T2-weighted MR images, it is likely a cyst or hemangioma, and the rest of the images in the study must be evaluated to characterize the lesion. If the liver contains innumerable distinctive nodules, an attempt should be made to look for nodules that are dominant because of size or differing signal intensity or attenuation compared with the background nodules. Distinctive nodulelike observations in cirrhosis include pseudomass and compensatory hypertrophy, large true nodules, steatotic nodules, siderotic nodules, T1-hyperintense nodules, and nodulelike arterial phase hyperenhancement. Specific appearances of distinctive nodular observations follow.

Pseudomass and Compensatory Hypertrophy

Definition—Pseudomasses are not true masses but are areas of hypertrophic liver parenchyma that may appear masslike compared with areas of fibrotic, atrophic liver (Fig. 19).

Findings—The pseudomass morphologic features may be seen with cirrhosis of any cause, primary sclerosing cholangitis (Fig. 19), Budd-Chiari syndrome, chronic portal vein obstruction, or sequela of severe acute hepatitis [36, 42–52]. The focal liver hypertrophy, often seen closer to the center of the liver or caudate lobe, may simulate a mass. These regions of hypertrophy follow the signal intensity and attenuation of normal liver, and the enhancement usually parallels that of normal noncirrhotic liver, without increased enhancement on arterial phase images, capsule appearance, or other features suggestive of HCC. Compared with surrounding fibrotic liver, the hypertrophic areas of regeneration generally have a closer to uniform appearance, lower signal intensity on T2-weighted images, higher signal intensity on T1-weighted images, similar or less enhancement during the arterial phase, and similar or lower signal intensity or attenuation on late phase images. Because the surrounding fibrotic regions often exhibit delayed phase enhancement, the area of hypertrophy may appear relatively hypointense or hypoattenuating by comparison (Fig. 20F).

LI-RADS categorization—The masslike appearance of hypertrophic liver parenchyma is most often associated with atrophic change and fibrosis in other portions of the liver. Most of these changes are categorized LI-RADS 1 or 2, depending on the radiologist's confidence level. Occasionally, if the imaging features are confusing, such entities may be categorized LI-RADS 3.

Large True Nodules

Definition—True large nodules (> 2 cm) (as opposed to compensatory hypertrophy) may be HCC or may represent a spectrum of benign hepatocellular nodules, including macroregenerative nodules (large regenerative nodules) and dysplastic nodules [2, 3, 53–55]. Dysplastic nodules are considered premalignant in the stepwise progression of hepatocarcinogenesis and therefore must be monitored closely. No imaging findings lead to a specific diagnosis of dysplastic nodule, but a constellation of findings may suggest this diagnosis.

Findings—Large nodules are usually well defined compared with background cirrhotic liver and may be isointense or hyperintense on T1-weighted images, isointense or hypointense on T2-weighted images, and be similarly enhancing or less enhancing on both arterial and delayed phase images.

LI-RADS categorization—Most large nodules are LI-RADS category 2 or 3 because they do not exhibit increased enhancement on arterial phase images, and they lack capsules and other features suggestive of HCC. A large true nodule that exhibits hyperenhancement in the arterial phase and washout in the portal venous or delayed phase can usually be categorized LI-RADS 4 or 5.

Steatotic Nodules

Definition—Steatotic nodules are nodules that contain more hepatocellular fat than the surrounding liver (Fig. 20). Intranodular steatosis more pronounced than steatosis of background liver may be seen in regenerative nodules but is frequently observed in dysplastic nodules and HCC [56, 57].

Findings—Imaging features of steatotic nodules include a masslike appearance; lower CT attenuation than background liver; loss of signal intensity on T1-weighted out-of-phase and fat-suppressed MR images compared with corresponding T1-weighted in-phase images; and an enhancement pattern identical to that of background liver over various phases of contrast enhancement (Fig. 20). If the pattern of enhancement is different over the phases, malignancy should be considered (Fig. 21). Detection of a steatotic nodule should prompt the radiologist to examine the pattern of enhancement of the nodule and additional ancillary features that may suggest malignancy. Focal fat deposition in liver parenchyma may have nodular morphologic features and mimic a steatotic nodule.

LI-RADS categorization—The LI-RADS categorization of steatotic nodules is the same as for nonsteatotic observations and depends on contrast enhancement characteristics and growth. The presence of fat alerts the reader to the observation but does not, by itself, determine the LI-RADS category. A

steatotic nodule can be assigned to LI-RADS category 2, 3, 4, or 5, depending on other features. A nodule that grows or becomes enhancing greater than background liver parenchyma in the arterial phase may be HCC and be assigned LI-RADS category 4 or 5.

Siderotic Nodules

Definition—A cirrhotic liver may have an increase in iron, either within discrete nodules—referred to as siderotic, or iron-rich, nodules—scattered through the liver diffusely in the parenchyma or, less commonly, in a periportal pattern. Siderotic nodules are usually benign (regenerative or dysplastic), although occasionally a focus of HCC may develop within a siderotic nodule [55, 58–60]. Nodules with iron have lower signal intensity on T2-weighted spin-echo or T2*-weighted gradient recalled-echo MR images. The signal intensity of siderotic nodules decreases more than that of adjacent unaffected liver because the TE is increased (Fig. 22). The presence of a masslike area of abnormal signal intensity that stands out against siderotic foci, or an iron-laden siderotic liver, should alert the reader to a focal mass (Fig. 23), which should be characterized further for assignment of a LI-RADS category. Siderotic nodules may be more difficult to detect at CT.

Findings—The imaging features of siderotic nodules include a masslike appearance, similar attenuation to or higher attenuation than surrounding liver on CT images; isointensity or hyperintensity on T1-weighted MR images with short TE; and hypointensity on T2- or T2*-weighted MR images with progressive loss of signal intensity with increasing TE (Fig. 22).

LI-RADS categorization—The LI-RADS classification of siderotic nodules is the same as for nonsiderotic observations and depends on contrast enhancement characteristics and growth. The presence of iron alerts the reader to the observation but does not, by itself, determine the LI-RADS category. It is rare for HCC to contain more iron than surrounding liver parenchyma. However, the development of a nonsiderotic component within a siderotic nodule may indicate an incident HCC and should be classified as LI-RADS category 3, 4, or 5 depending on size, growth, and enhancement features.

T1-Hyperintense Nodules

Definition—T1-hyperintense nodules have a shorter T1 relaxation time than background liver and so have higher signal intensity on T1-weighted images, even with fat suppression (Fig. 24). The mechanism of the shorter T1 relaxation time has not been defined, but the presence of hemorrhage, copper, iron, and other paramagnetic materials has been noted [61–65]. T1-hyperintense nodules may be regenerative, dysplastic, or malignant (Fig. 25).

Findings—T1-hyperintense nodules have higher signal intensity on T1-weighted images than does background liver with no loss of signal intensity on T1-weighted out-of-phase images compared with T1-weighted in-phase images or with the use of fat suppression (Figs. 24 and 25). Assessment of the pattern of enhancement of these lesions with high signal intensity on unenhanced T1-weighted images may be challenging but is critical in assigning a LI-RADS category. Subtraction images may be helpful if there is no significant misregistration artifact.

LI-RADS categorization—The LI-RADS categorization of T1-hyperintense nodules depends on other features, such as contrast enhancement characteristics and growth. The presence of increased signal intensity on T1-weighted images alerts the reader to the observation but does not, by itself, determine the LI-RADS category. This appearance by itself can therefore be assigned to LI-RADS category 2, 3, 4, or 5, depending on other features.

Nodulelike Arterial Phase Hyperenhancement

Definition—Nodulelike arterial phase hyperenhancement (NAPH) is less than 20 mm of hyperenhancement with a nodular configuration and visible only in the arterial phase. NAPH is thought to usually represent either a perfusion alteration or a small nonmalignant mass (e.g., hyperplastic lesion, hemangioma, dysplastic nodule) but occasionally represents a small HCC [41, 66–69].

Findings—NAPH is a round or near-round focus of enhancement (Fig. 26). This observation is invisible on all unenhanced and later phase images and may represent an arterioportal shunt, especially if it is at the periphery of the liver or has a slightly elongated shape. However, HCC can have the same imaging appearance (Fig. 27). HCC is commonly seen as an arterial phase hyperenhancing nodule. For this reason, careful assessment for other associated findings (e.g., T2 hyperintensity, diminished signal intensity or attenuation on delayed images, capsule appearance, restricted diffusion) should be performed. Hyperplastic nodules are well defined and exhibit intense enhancement on arterial phase images. They are usually subtle or invisible on other images. They may retain hepatobiliary contrast agent in later phases.

LI-RADS categorization—Most areas of NAPH smaller than 1 cm and not visible on other images (as they are defined) represent benign conditions (e.g., arterioportal shunt or hyperplastic nodule). Larger size and other suspicious ancillary features (e.g., T2 hyperintensity, diminished signal intensity or attenuation on delayed images, capsule appearance) increase the likelihood of HCC. Therefore, NAPH can be categorized LI-RADS 2, 3, or 4, depending on other features.

Hyperplastic nodules are benign. They are common in underlying diseases that severely alter perfusion, such as Budd-Chiari syndrome and, less commonly, chronic portal venous occlusion and large arterioportal fistula [68, 69]. Given their enhancement pattern, these nodules may be difficult to differentiate from HCC. Many therefore are categorized LI-RADS 3 or 4. If a well-defined homogeneously hyperenhancing (other than possible central scar) nodule without a capsule appearance remains stable for longer than 1 year, particularly in a patient with the underlying conditions described, a diagnosis of benign hyperplastic nodule becomes increasingly likely. The LI-RADS category may therefore evolve from 4 to 3, or occasionally to 2. Conversely, if the patient presents with a history of viral hepatitis, alcoholism, nonalcoholic steatohepatitis, or other chronic liver disease, NAPH should be followed to ensure it does not represent HCC or its precursors.

Conclusion

Imaging is currently used for diagnosis, staging, and triage of patients with HCC. LI-RADS has been developed to standardize the interpretation and reporting of liver observations in patients at risk of HCC. Understanding of features considered benign or likely benign in a cirrhotic liver is important to reducing imaging interpretation variability and errors. This review exposes radiologists to the LI-RADS terminology and provides a comprehensive list of imaging features that favor benignity, allowing appropriate care of patients at risk of HCC.

References

1. American College of Radiology website. Liver Imaging Reporting and Data System. www.acr.org/Quality-Safety/Resources/LIRADS. Accessed March 21, 2014
2. Hanna RF, Aguirre DA, Kased N, Emery SC, Pe-

terson MR, Sirlin CB. Cirrhosis-associated hepatocellular nodules: correlation of histopathologic and MR imaging features. *RadioGraphics* 2008; 28:747–769

3. Willatt JM, Hussain HK, Adusumilli S, Marrero JA. MR imaging of hepatocellular carcinoma in the cirrhotic liver: challenges and controversies. *Radiology* 2008; 247:311–330
4. Coleman WB. Mechanisms of human hepatocarcinogenesis. *Curr Mol Med* 2003; 3:573–588
5. Efremidis SC, Hytiroglou P. The multistep process of hepatocarcinogenesis in cirrhosis with imaging correlation. *Eur Radiol* 2002; 12:753–764
6. Bruix J, Sherman M. Management of hepatocellular carcinoma: an update. *Hepatology* 2011; 53:1020–1022
7. European Association for the Study of the Liver; European Organisation for Research and Treatment of Cancer. EASL-EORTC clinical practice guidelines: management of hepatocellular carcinoma. *J Hepatol* 2012; 56:908–943
8. Song P, Tobe RG, Inagaki Y, et al. The management of hepatocellular carcinoma around the world: a comparison of guidelines from 2001 to 2011. *Liver Int* 2012; 32:1053–1063
9. Wald C, Russo MW, Heimbach JK, Hussain HK, Pomfret EA, Bruix J. New OPTN/UNOS policy for liver transplant allocation: standardization of liver imaging, diagnosis, classification, and reporting of hepatocellular carcinoma. *Radiology* 2013; 266:376–382
10. Pomfret EA, Washburn K, Wald C, et al. Report of a national conference on liver allocation in patients with hepatocellular carcinoma in the United States. *Liver Transpl* 2010; 16:262–278
11. U.S. Department of Health and Human Services, Organ Procurement and Transplantation website. Policy 9: allocation of livers and liver-intestines. optn.transplant.hrsa.gov/ContentDocuments/OPTN_Policies.pdf. Accessed March 21, 2014
12. Saxena R. Premalignant hepatocellular lesions. In: *Practical hepatic pathology: a diagnostic approach*. Philadelphia, PA: Elsevier/Saunders, 2011:457–472
13. Baron RL, Campbell WL, Dodd GD III. Peribiliary cysts associated with severe liver disease: imaging-pathologic correlation. *AJR* 1994; 162:631–636
14. Dodd GD, Baron RL, Oliver JH 3rd, Federle MP. Spectrum of imaging findings of the liver in end-stage cirrhosis. Part II. Focal abnormalities. *AJR* 1999; 173:1185–1192
15. Brancatelli G, Federle MP, Blachar A, Grazioli L. Hemangioma in the cirrhotic liver: diagnosis and natural history. *Radiology* 2001; 219:69–74
16. Caturelli E, Pompili M, Bartolucci F, et al. Hemangioma-like lesions in chronic liver disease: diagnostic evaluation in patients. *Radiology* 2001; 220:337–342
17. Kamel IR, Liapi E, Fishman EK. Incidental non-neoplastic hypervascular lesions in the noncirrhotic liver: diagnosis with 16-MDCT and 3D CT angiography. *AJR* 2006; 187:682–687
18. Lee SJ, Lim JH, Lee WJ, Lim HK, Chao SW, Choo IW. Transient subsegmental hepatic parenchymal enhancement on dynamic CT: a sign of postbiopsy arterioportal shunt. *J Comput Assist Tomogr* 1997; 21:355–360
19. Larson AM. Liver disease in hereditary hemorrhagic telangiectasia. *J Clin Gastroenterol* 2003; 36:149–158
20. Buscarini E, Plauchu H, Garcia Tsao G, et al. Liver involvement in hereditary hemorrhagic telangiectasia: consensus recommendations. *Liver Int* 2006; 26:1040–1046
21. Itai Y, Matsui O. Blood flow and liver imaging. *Radiology* 1997; 202:306–314
22. Schlund JF, Semelka RC, Kettritz U, Eisenberg LB, Lee JK. Transient increased segmental hepatic enhancement distal to portal vein obstruction on dynamic gadolinium-enhanced gradient-echo MR images. *J Magn Reson Imaging* 1995; 5:375–377
23. Ito K, Honjo K, Fujita T, Awaya H, Matsumoto T, Matsunaga N. Hepatic parenchymal hyperperfusion abnormalities detected with multisection dynamic MR imaging: appearance and interpretation. *J Magn Reson Imaging* 1996; 6:861–867
24. Shimizu A, Ito K, Koike S, Fujita T, Shimizu K, Matsunaga N. Cirrhosis or chronic hepatitis: evaluation of small (≤2-cm) early enhancing hepatic lesions with serial contrast-enhanced dynamic MR imaging. *Radiology* 2003; 226:550–555
25. Colagrande S, Centi N, Galdiero R, Ragozzino A. Transient hepatic intensity differences. Part II. Those not associated with focal lesions. *AJR* 2007; 188:160–166
26. Lautt WW. Mechanism and role of intrinsic regulation of hepatic arterial blood flow: hepatic arterial buffer response. *Am J Physiol* 1985; 249:G549–G556
27. Eipel C, Abshagen K, Vollmar B. Regulation of hepatic blood flow: the hepatic arterial buffer response revisited. *World J Gastroenterol* 2010; 16:6046–6057
28. Hamer OW, Aguirre DA, Casola G, Lavine JE, Woenckhaus M, Sirlin CB. Fatty liver: imaging patterns and pitfalls. *RadioGraphics* 2006; 26:1637–1653
29. Karcaaltincaba M, Akhan O. Imaging of hepatic steatosis and fatty sparing. *Eur J Radiol* 2007; 61:33–43
30. Hamer OW, Aguirre DA, Casola G, Sirlin CB. Imaging features of perivascular fatty infiltration of the liver: initial observations. *Radiology* 2005; 237:159–169
31. Jacobs JE, Birnbaum BA, Shapiro MA, et al. Diagnostic criteria for fatty infiltration of the liver on contrast-enhanced helical CT. *AJR* 1998; 171:659–664
32. Venkataraman S, Braga L, Semelka RC. Imaging the fatty liver. *Magn Reson Imaging Clin N Am* 2002; 10:93–103
33. Kemper J, Jung G, Poll LW, Jonkmanns C, Lüthen R, Moedder U. CT and MRI findings of multifocal hepatic steatosis mimicking malignancy. *Abdom Imaging* 2002; 27:708–710
34. Brancatelli G, Federle MP, Baron RL, Lagalla R, Midiri M, Vilgrain V. Arterially enhancing liver lesions: significance of sustained enhancement on hepatic venous and delayed phase with magnetic resonance imaging. *J Comput Assist Tomogr* 2007; 31:116–124
35. Baron RL, Peterson MS. From the RSNA refresher courses: screening the cirrhotic liver for hepatocellular carcinoma with CT and MR imaging—opportunities and pitfalls. *RadioGraphics* 2001; 21:S117–S132
36. Dodd GD, Baron RL, Oliver JH 3rd, Federle MP. Spectrum of imaging findings of the liver in end-stage cirrhosis. Part I. Gross morphology and diffuse abnormalities. *AJR* 1999; 173:1031–1036
37. Ahn IO, de Lange EE. Early hyperenhancement of confluent hepatic fibrosis on dynamic MR imaging. *AJR* 1998; 171:901–902
38. Choi BI, Lee JM, Han JK. Imaging of intrahepatic and hilar cholangiocarcinoma. *Abdom Imaging* 2004; 29:548–557
39. Blachar A, Federle MP, Brancatelli G. Hepatic capsular retraction: spectrum of benign and malignant etiologies. *Abdom Imaging* 2002; 27:690–699
40. Jeong YY, Mitchell DG, Kamishima T. Small (<20 mm) enhancing hepatic nodules seen on arterial phase MR imaging of the cirrhotic liver: clinical implications. *AJR* 2002; 178:1327–1334
41. Holland AE, Hecht EM, Hahn WY, et al. Importance of small (< or = 20-mm) enhancing lesions seen only during the hepatic arterial phase at MR imaging of the cirrhotic liver: evaluation and comparison with whole explanted liver. *Radiology* 2005; 237:938–944
42. Kim TK, Chung JW, Han JK, Kim AY, Park JH, Choi BI. Hepatic changes in benign obstruction of the hepatic inferior vena cava: CT findings. *AJR* 1999; 173:1235–1242
43. Tublin ME, Towbin AJ, Federle MP, Nalesnik MA. Altered liver morphology after portal vein thrombosis: not always cirrhosis. *Dig Dis Sci* 2008; 53:2784–2788
44. Vilgrain V, Condat B, Bureau C, et al. Atrophy-hypertrophy complex in patients with cavernous transformation of the portal vein: CT evaluation. *Radiology* 2006; 241:149–155
45. Lory J, Schweizer W, Blumgart LH, Zimmer-

mann A. The pathology of the atrophy/hypertrophy complex (AHC) of the liver: a light microscopic and immunohistochemical study. *Histol Histopathol* 1994; 9:541–554
46. Ito K, Mitchell DG, Outwater EK, Blasbalg R. Primary sclerosing cholangitis: MR imaging features. *AJR* 1999; 172:1527–1533
47. Okazaki H, Ito K, Fujita T, Koike S, Takano K, Matsunaga N. Discrimination of alcoholic from virus-induced cirrhosis on MR imaging. *AJR* 2000; 175:1677–1681
48. Dodd GD, Baron RL, Oliver JH, Federle MP. End-stage primary sclerosing cholangitis: CT findings of hepatic morphology in 36 patients. *Radiology* 1999; 211:357–362
49. Bader TR, Beavers KL, Semelka RC. MR imaging features of primary sclerosing cholangitis: patterns of cirrhosis in relationship to clinical severity of disease. *Radiology* 2003; 226:675–685
50. Blachar A, Federle M, Brancatelli G. Primary biliary cirrhosis: clinical, pathologic, and helical CT findings in 53 patients. *Radiology* 2001; 220:329–336
51. Mitchell DG, Palazzo J, Hann HW, et al. Mass-like hepatic hypertrophy: MRI findings with histologic correlation. *Magn Reson Imaging* 1992; 10:541–547
52. Brancatelli G, Federle MP, Grazioli L, Golfieri R, Lencioni R. Large regenerative nodules in Budd-Chiari syndrome and other vascular disorders of the liver: CT and MR imaging findings with clinicopathologic correlation. *AJR* 2002; 178:877–883
53. Borzio M, Fargion S, Borzio F, et al. Impact of large regenerative, low grade and high grade dysplastic nodules in hepatocellular carcinoma development. *J Hepatol* 2003; 39:208–214
54. Roncalli M. Hepatocellular nodules in cirrhosis: focus on diagnostic criteria on liver biopsy—a Western experience. *Liver Transpl* 2004; 10:S9–S15
55. Krinsky GA, Lee VS. MR imaging of cirrhotic nodules. *Abdom Imaging* 2000; 25:471–482
56. Yu JS, Chung JJ, Kim JH, Kim KW. Fat-containing nodules in the cirrhotic liver: chemical shift MRI features and clinical implications. *AJR* 2007; 188:1009–1016
57. Prasad SR, Wang H, Rosas H, et al. Fat-containing lesions of the liver: radiologic-pathologic correlation. *RadioGraphics* 2005; 25:321–331
58. Krinsky GA, Lee VS, Nguyen MT, et al. Siderotic nodules in the cirrhotic liver at MR imaging with explant correlation: no increased frequency of dysplastic nodules and hepatocellular carcinoma. *Radiology* 2001; 218:47–53
59. Zhang J, Krinsky GA. Iron-containing nodules of cirrhosis. *NMR Biomed* 2004; 17:459–464
60. Ito K, Mitchell DG, Gabata T, et al. Hepatocellular carcinoma: association with increased iron deposition in the cirrhotic liver at MR imaging. *Radiology* 1999; 212:235–240
61. Ebara M, Fukuda H, Kojima Y, et al. Small hepatocellular carcinoma: relationship of signal intensity to histopathologic findings and metal content of the tumor and surrounding hepatic parenchyma. *Radiology* 1999; 210:81–88
62. Earls JP, Theise ND, Weinreb JC, et al. Dysplastic nodules and hepatocellular carcinoma: thin-section MR imaging of explanted cirrhotic livers with pathologic correlation. *Radiology* 1996; 201:207–214
63. Honda H, Kaneko K, Kanazawa Y, et al. MR imaging of hepatocellular carcinomas: effect of Cu and Fe contents on signal intensity. *Abdom Imaging* 1997; 22:60–66
64. Mitchell DG, Palazzo J, Hann H, Rifkin MD, Burk DL, Rubin R. Hepatocellular tumors with high signal on T1-weighted MR imaging: chemical shift MR imaging and histologic correlation. *J Comput Assist Tomogr* 1991; 15:762–769
65. Kelekis NL, Semelka RC, Woosley JT. Malignant lesions of the liver with high signal intensity on T1-weighted MR images. *J Magn Reson Imaging* 1996; 6:291–294
66. Matsui O, Kadoya M, Kameyama T, et al. Benign and malignant nodules in cirrhotic livers: distinction based on blood supply. *Radiology* 1991; 178:493–497
67. Marrero JA, Hussain HK, Nghiem HV, Umar R, Fontana RJ, Lok AS. Improving the prediction of hepatocellular carcinoma in cirrhotic patients with an arterially-enhancing liver mass. *Liver Transpl* 2005; 11:281–289
68. Reshamwala PA, Kleiner DE, Heller T. Nodular regenerative hyperplasia: not all nodules are created equal. *Hepatology* 2006; 44:7–14
69. Vilgrain V, Lewin M, Vons C, et al. Hepatic nodules in Budd-Chiari syndrome: imaging features. *Radiology* 1999; 210:443–450

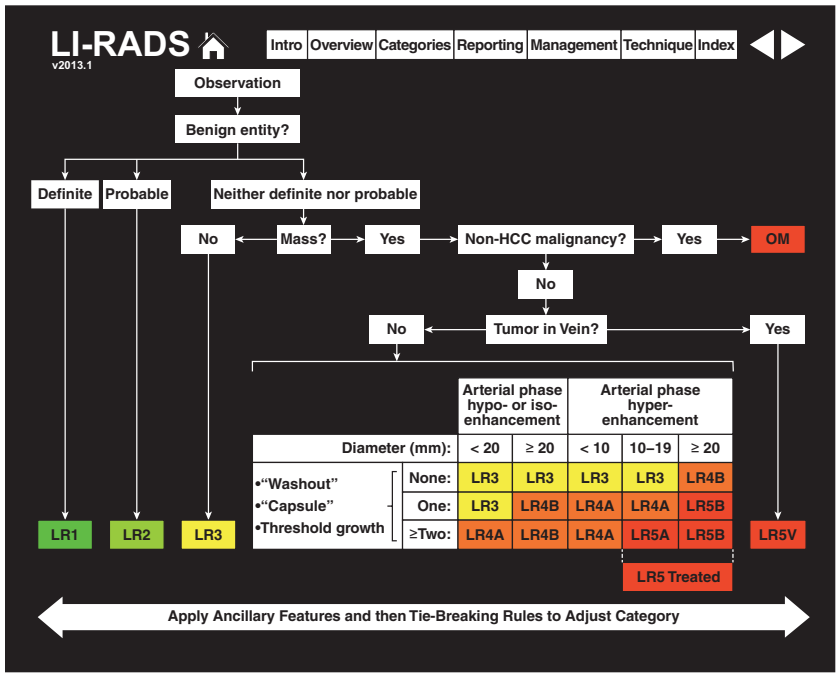

Fig. 1—Chart shows Liver Imaging Reporting and Data System (LI-RADS) categories. HCC = hepatocellular carcinoma, OM = other malignancy, LR = LI-RADS, V = venous. Reprinted with permission of the American College of Radiology. Liver Imaging Reporting and Data System version 2013.1. Accessed March 2014, from www.acr.org/Quality-Safety/Resources/LIRADS. No other representation of this material is authorized without expressed, written permission from the American College of Radiology.

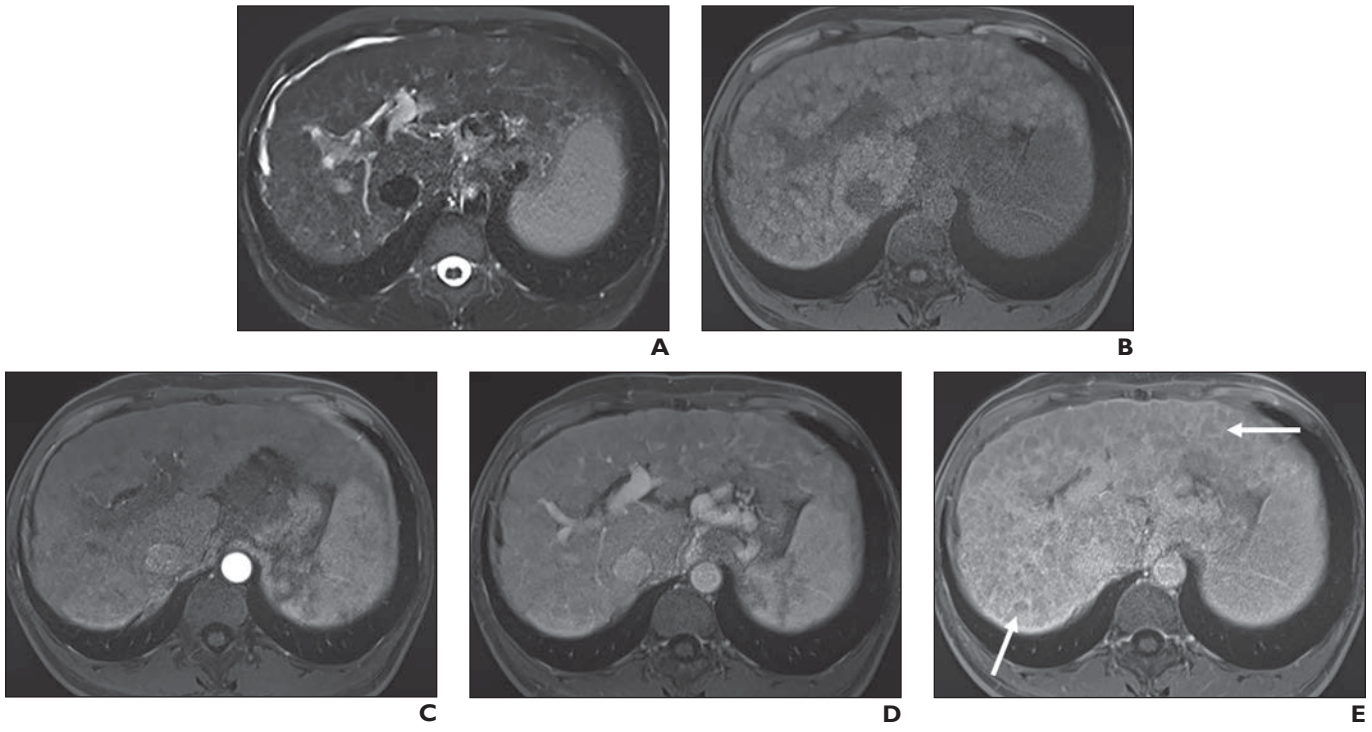

Fig. 2—60-year-old woman with hepatitis C cirrhosis. Example of typical cirrhotic nodules. Multiple subcentimeter nodules are present throughout liver parenchyma and are close to uniform in size and signal intensity. These are often best seen as discrete nodules on delayed phase images, because areas of underlying fibrosis exhibit delayed enhancement.
A, T2-weighted MR image.
B, Unenhanced fat-suppressed T1-weighted MR image.
C, Arterial phase fat-suppressed T1-weighted MR image.
D, Portal venous phase fat-suppressed T1-weighted MR image.
E, Five-minute delayed venous phase fat-suppressed T1-weighted image (*arrows*).

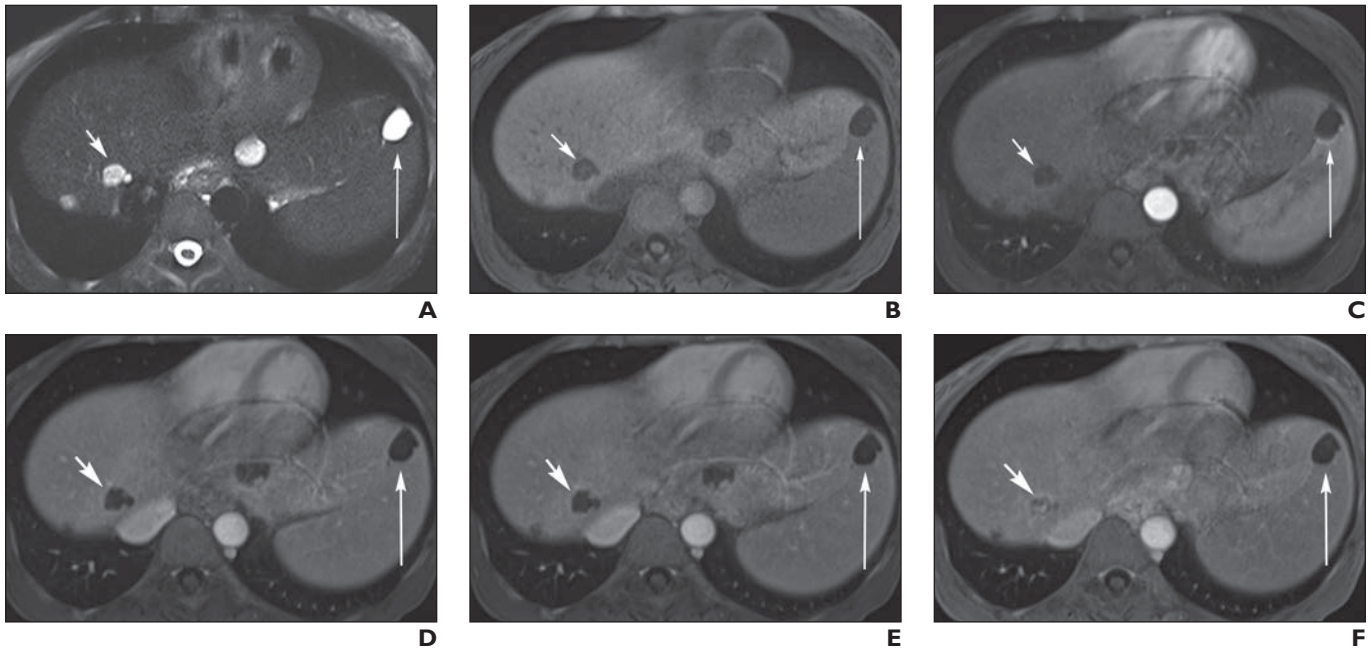

Fig. 3—48-year-old woman with hepatitis C undergoing imaging for routine surveillance. Example of hepatic cyst and typical hemangiomas. Lesions without enhancement are cysts (*long arrow*). Others with peripheral nodular enhancement have centripetal filling, which is typical enhancement pattern for typical hemangioma (*short arrow*).
A, T2-weighted MR image shows multiple lesions with high signal intensity.
B, Unenhanced fat-suppressed T1-weighted MR image.
C, Arterial phase T1-weighted fat-suppressed MR image.
D, Portal venous phase T1-weighted fat-suppressed MR image.
E, Three-minute delayed venous phase fat-suppressed T1-weighted image.
F, Five-minute delayed venous phase fat-suppressed T1-weighted image.

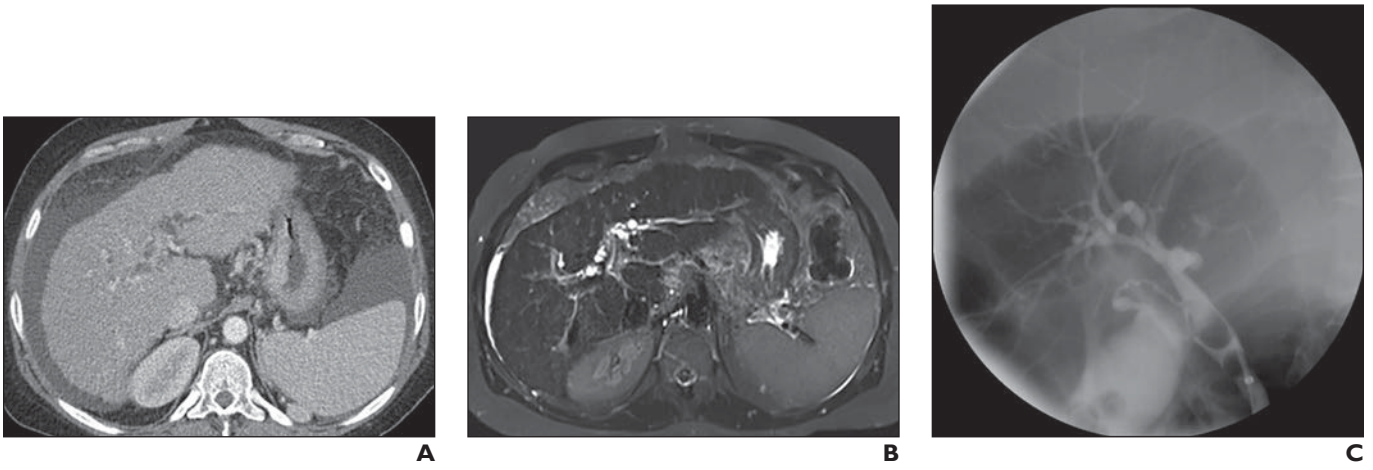

Fig. 4—60-year-old man with hepatitis C cirrhosis with areas of irregular tubular fluid attenuation and signal intensity along central periportal region. Example of peribiliary cysts, which have appearance of dilated bile ducts. However, more peripheral bile ducts are not dilated.
A, Contrast-enhanced CT image.
B, T2-weighted MR image.
C, ERCP image shows bile ducts are smooth and nondilated, as expected with peribiliary cysts, which do not communicate with biliary system.

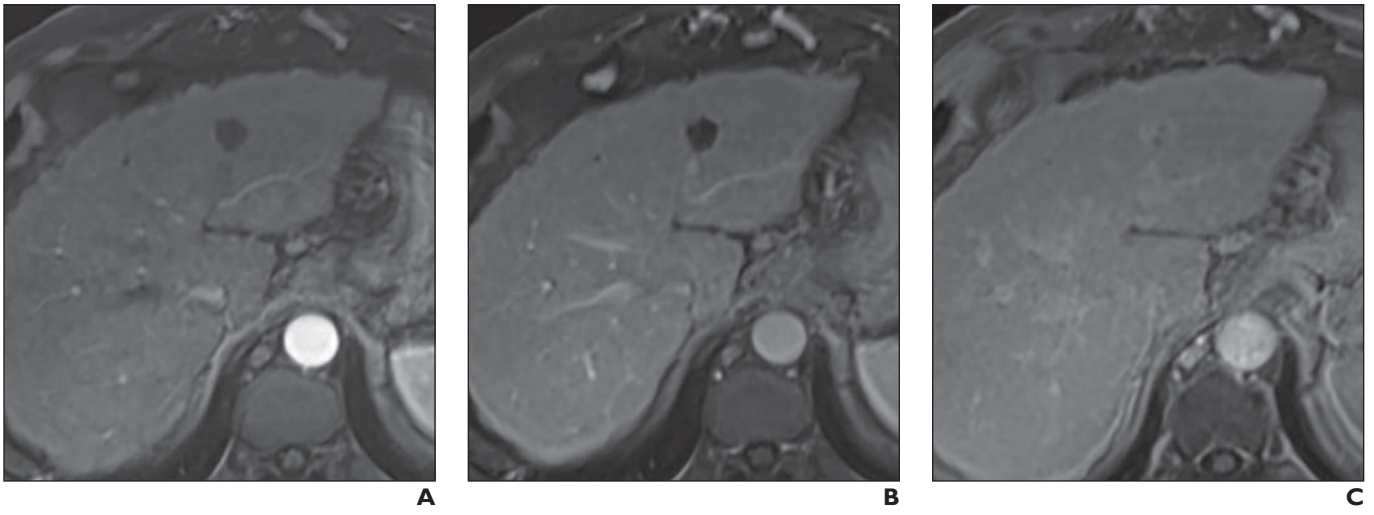

Fig. 5—68-year-old man with cirrhosis. Example of hemangiomas with atypical enhancement patterns. Well-defined lesion in segment II had high signal intensity on T2-weighted MR images (not shown), low signal intensity on T1-weighted images (not shown), and minimally nodular enhancement on several immediate contrast-enhanced images with definite central filling in on late-phase images. This pattern of enhancement may be seen in both noncirrhotic and cirrhotic livers.
A, Arterial phase fat-suppressed T1-weighted MR image.
B, Portal venous phase fat-suppressed T1-weighted MR image.
C, Five-minute delayed venous phase fat-suppressed T1-weighted image.

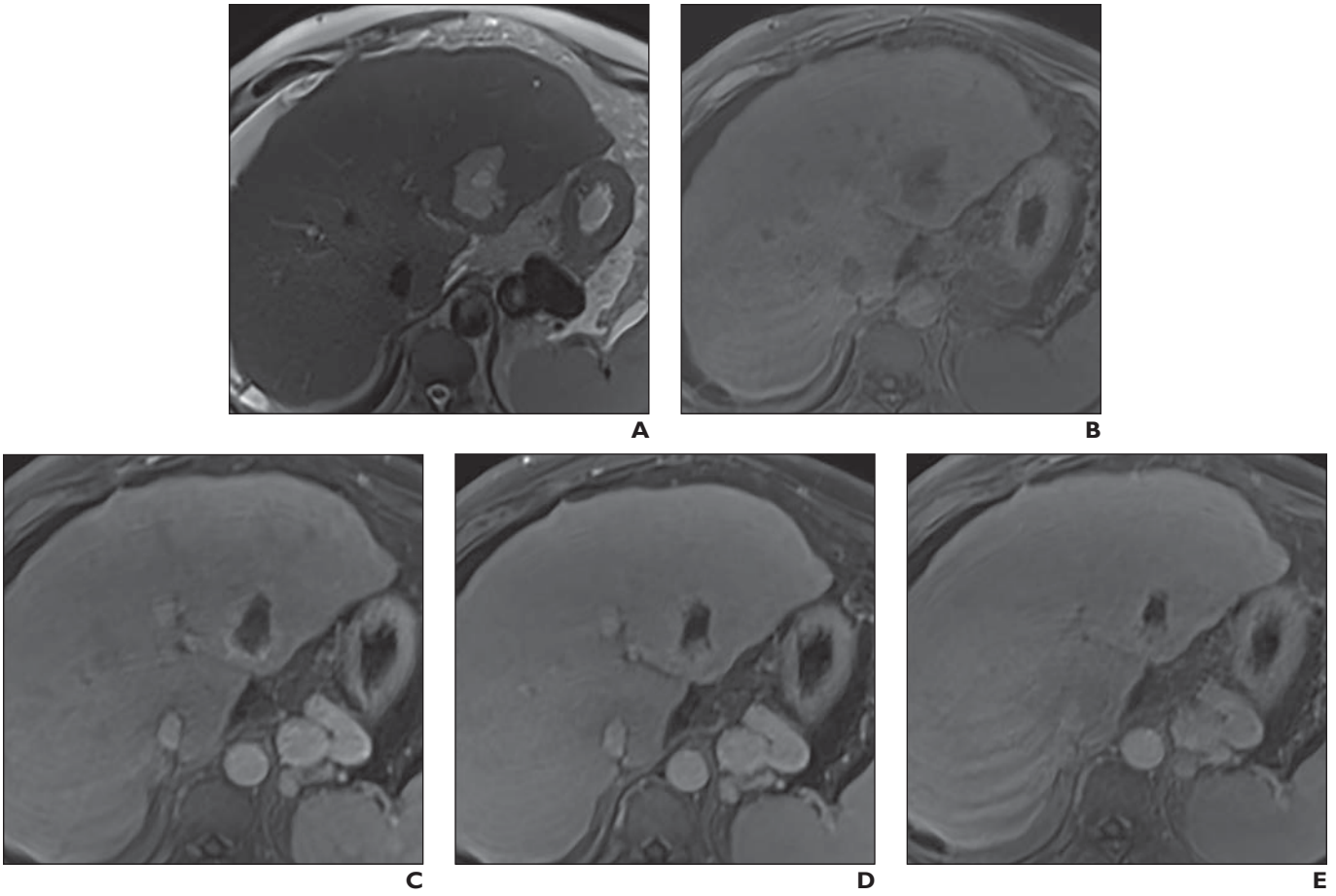

Fig. 6—55-year-old man with alcoholic cirrhosis with hepatocellular carcinoma diagnosed on outside study. Example of hemangioma with ringlike enhancement. Dominant mass in segment II–III has lobulate contour, high signal intensity on T2-weighted image with central focus of even higher signal intensity, and corresponding diminished signal intensity on T1-weighted image. After contrast infusion, there is continuous rim of enhancement, which exhibits centripetal filling on late phase images without complete filling of central portion. This pattern of enhancement may be seen in cirrhotic liver and is likely related to fibrosis around fluid-filled hemangioma and to early hyalinization.
A, T2-weighted MR image shows high signal intensity of mass with central focus of even higher signal intensity.
B, Unenhanced fat-suppressed T1-weighted image shows diminished signal intensity corresponding to **A.**
C, Arterial phase fat-suppressed T1-weighted MR image.
D, Portal venous phase fat-suppressed T1-weighted MR image.
E, Five-minute delayed venous phase fat-suppressed T1-weighted image.

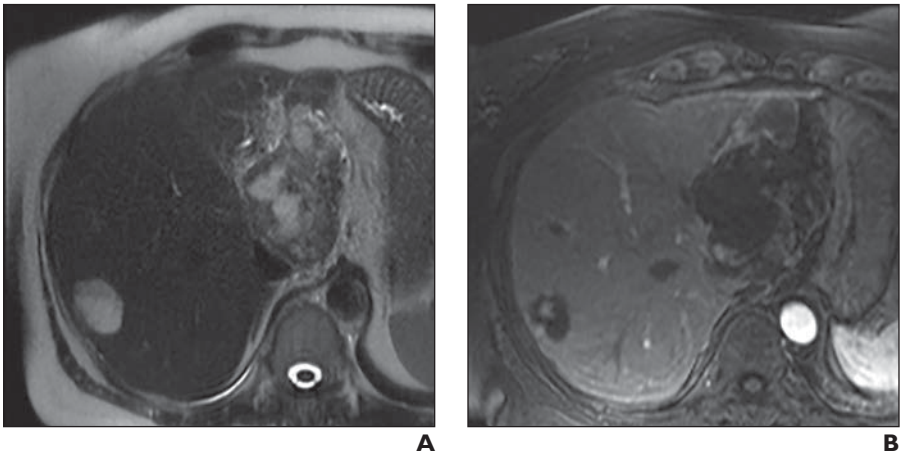

Fig. 7—57-year-old woman with nonalcoholic fatty liver disease. Example of hyalinized hemangioma. Initial images (**A**–**D**) show one lesion present in segment VI and one exophytic lesion arising from segment IVB in porta hepatis. Segment VI lesion has high signal intensity on T2-weighted image (**A**), whereas exophytic lesion is more complex, with areas of lower signal intensity in its periphery and interspersed in its center. Both lesions had diminished signal intensity on T1-weighted images (not shown) and nodular interrupted peripheral enhancement with centripetal filling on later phase contrast-enhanced images (**B**–**D**). Four years later (**E**–**H**), changes likely related to hyalinization of hemangiomas are present. Both lesions (*arrows*, **E**–**H**) are smaller than earlier examination (**A**–**D**), less well defined, have lower signal intensity on T2-weighted images, and have less classic enhancement pattern on early phases after contrast material administration (**F** and **G**) with filling in on 5-minute delayed phase image (**H**).
A, Initial T2-weighted MR image.
B, Initial arterial phase fat-suppressed T1-weighted MR image.

(Fig. 7 continues on next page)

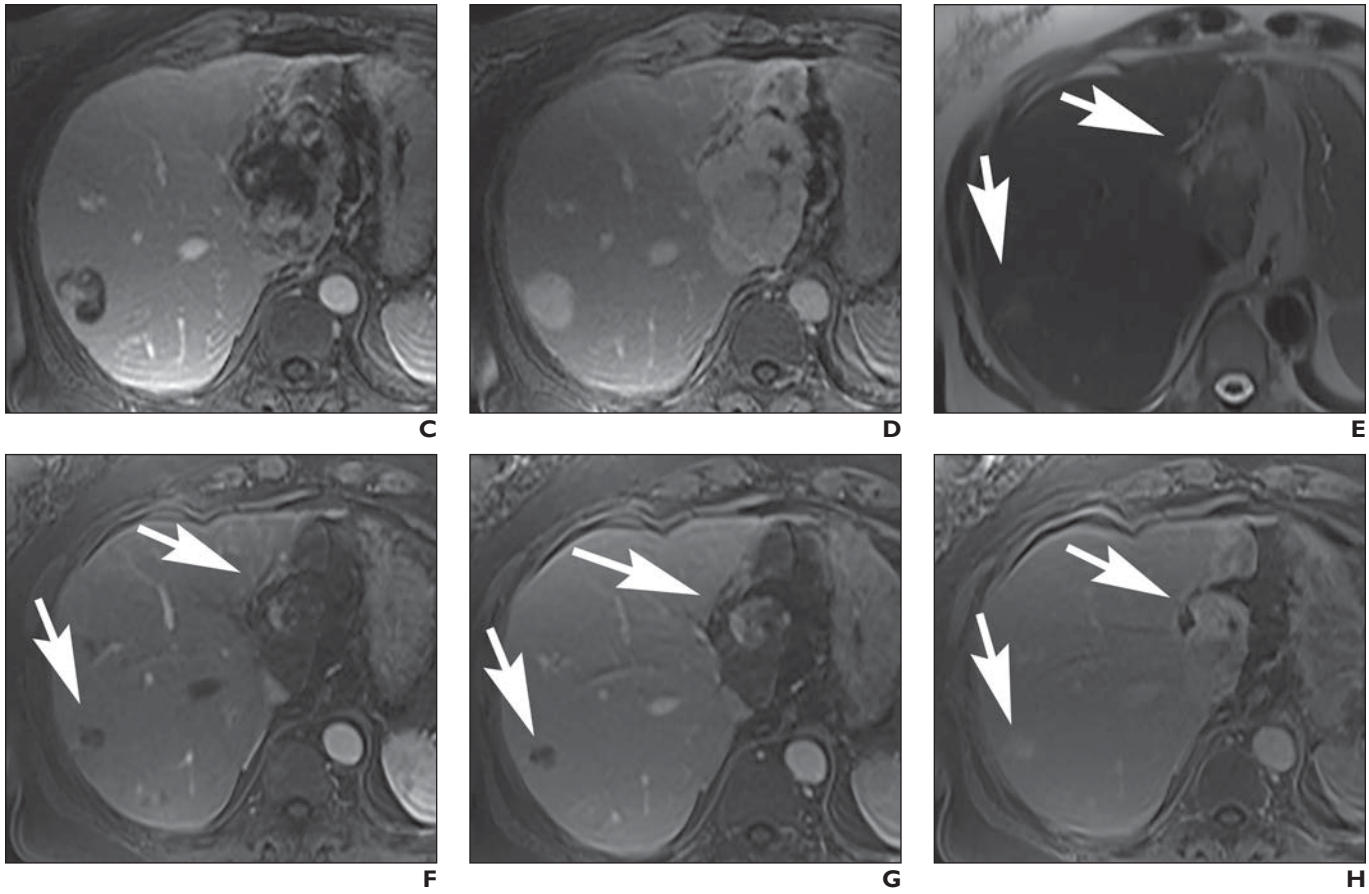

Fig. 7 (continued)—57-year-old woman with nonalcoholic fatty liver disease. Example of hyalinized hemangioma. Initial images (**A**–**D**) show one lesion present in segment VI and one exophytic lesion arising from segment IVB in porta hepatis. Segment VI lesion has high signal intensity on T2-weighted image (**A**), whereas exophytic lesion is more complex, with areas of lower signal intensity in its periphery and interspersed in its center. Both lesions had diminished signal intensity on T1-weighted images (not shown) and nodular interrupted peripheral enhancement with centripetal filling on later phase contrast-enhanced images (**B**–**D**). Four years later (**E**–**H**), changes likely related to hyalinization of hemangiomas are present. Both lesions (*arrows*, **E**–**H**) are smaller than earlier examination (**A**–**D**), less well defined, have lower signal intensity on T2-weighted images, and have less classic enhancement pattern on early phases after contrast material administration (**F** and **G**) with filling in on 5-minute delayed phase image (**H**).
C, Initial portal venous phase fat-suppressed T1-weighted MR image.
D, Initial 5-minute delayed venous phase fat-suppressed T1-weighted MR image.
E, Follow-up T2-weighted MR image obtained 4 years after **A**.
F, Follow-up arterial phase fat-suppressed T1-weighted MR image obtained 4 years after **B**.
G, Follow-up portal venous phase fat-suppressed T1-weighted MR image obtained 4 years after **C**.
H, Follow-up 5-minute delayed venous phase fat-suppressed T1-weighted MR image obtained 4 years after **D**.

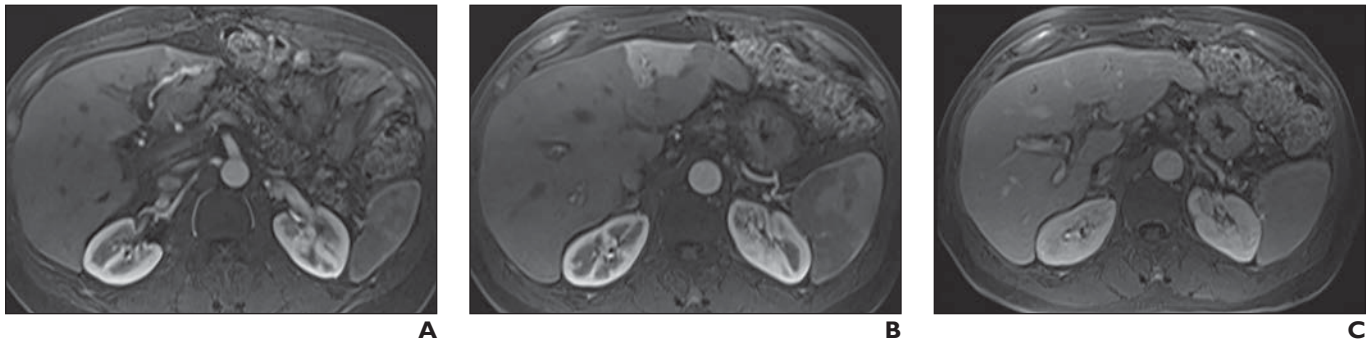

Fig. 8—59-year-old man with small arteriovenous fistula and previous biopsy. Example of vascular abnormalities. Triangular area of arterial phase hyperenhancement (transient hepatic intensity difference) in segment II equilibrates in portal venous phase. In segment II–III, small focal area of dilated anomalous connection between hepatic artery and portal vein represents small arteriovenous fistula. Patient had undergone ultrasound-guided liver biopsy in vicinity 2 months earlier.
A, Arterial phase fat-suppressed T1-weighted MR image in segment II–III.
B, Arterial phase fat-suppressed T1-weighted MR image in segment II.
C, Portal venous phase fat-suppressed T1-weighted MR image in segment II.

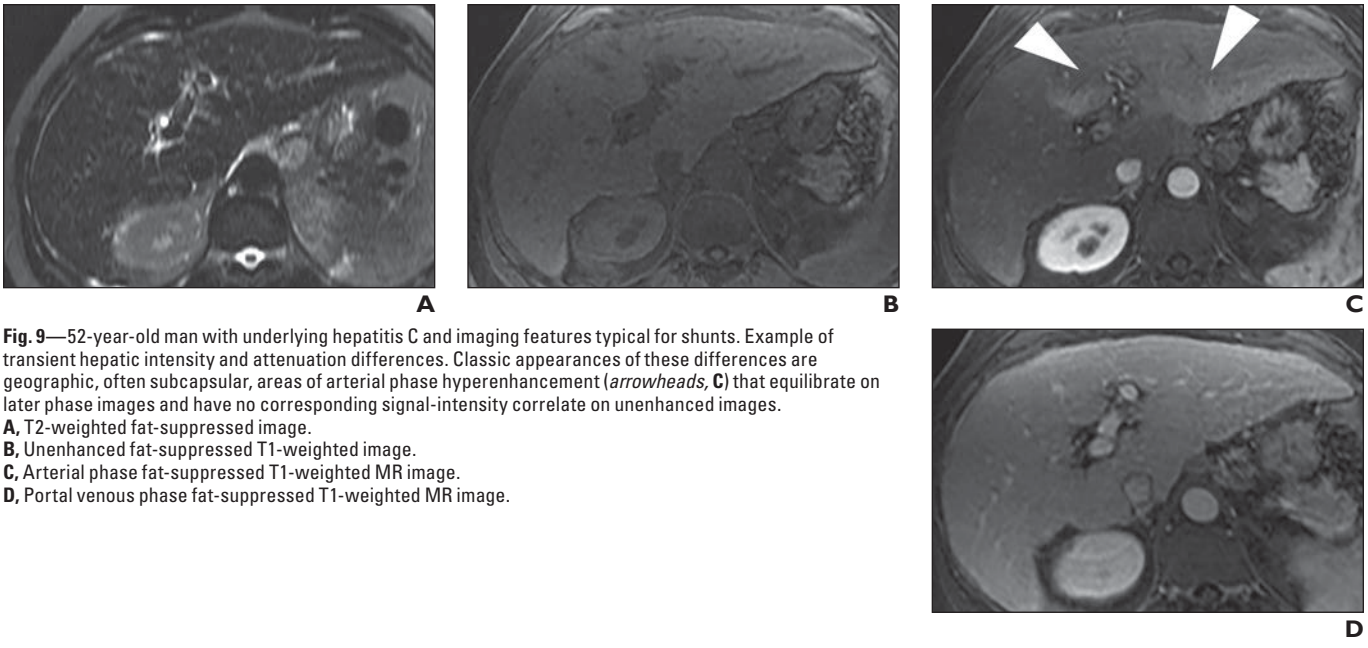

Fig. 9—52-year-old man with underlying hepatitis C and imaging features typical for shunts. Example of transient hepatic intensity and attenuation differences. Classic appearances of these differences are geographic, often subcapsular, areas of arterial phase hyperenhancement (*arrowheads,* **C**) that equilibrate on later phase images and have no corresponding signal-intensity correlate on unenhanced images.
A, T2-weighted fat-suppressed image.
B, Unenhanced fat-suppressed T1-weighted image.
C, Arterial phase fat-suppressed T1-weighted MR image.
D, Portal venous phase fat-suppressed T1-weighted MR image.

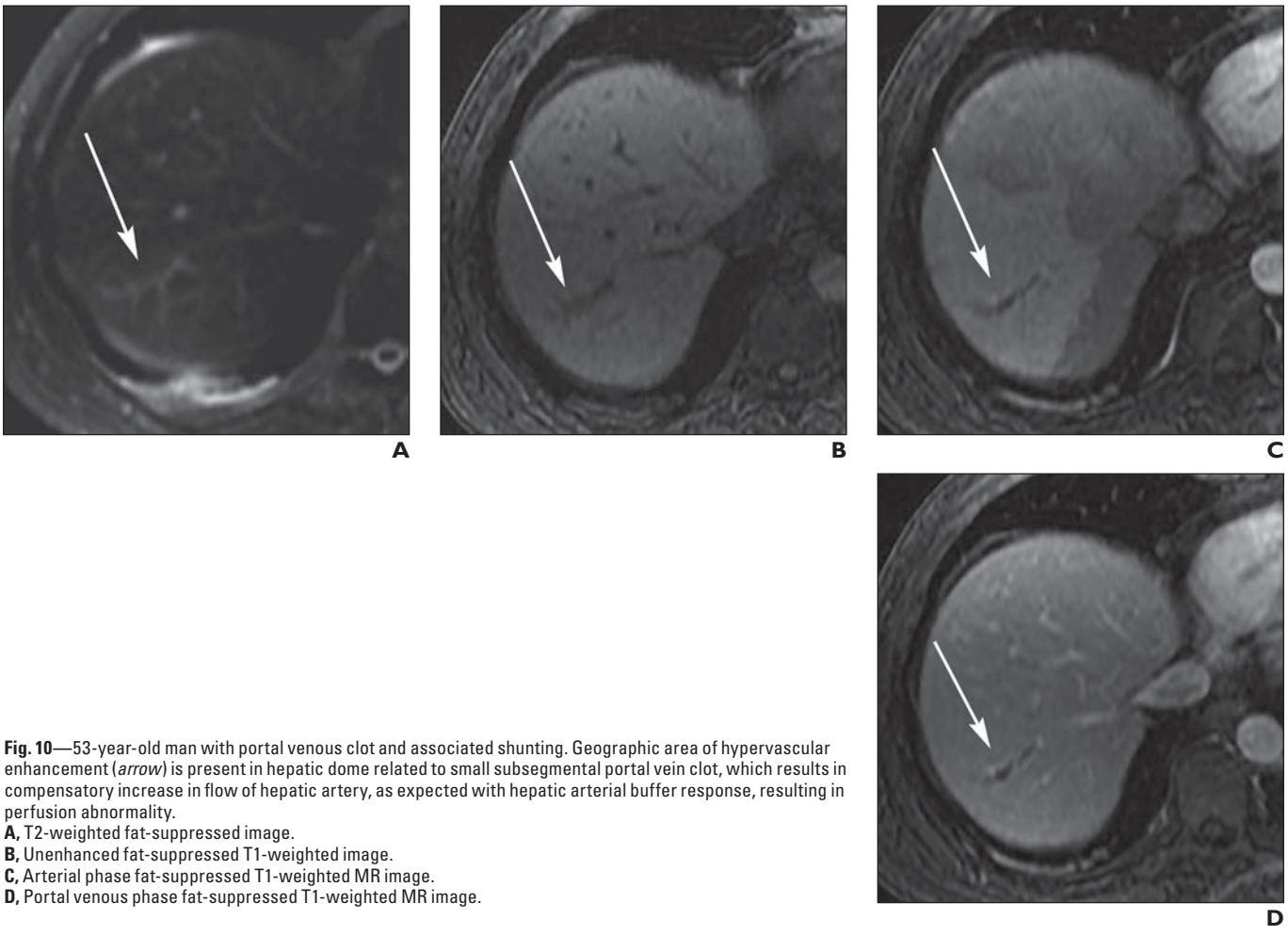

Fig. 10—53-year-old man with portal venous clot and associated shunting. Geographic area of hypervascular enhancement (*arrow*) is present in hepatic dome related to small subsegmental portal vein clot, which results in compensatory increase in flow of hepatic artery, as expected with hepatic arterial buffer response, resulting in perfusion abnormality.
A, T2-weighted fat-suppressed image.
B, Unenhanced fat-suppressed T1-weighted image.
C, Arterial phase fat-suppressed T1-weighted MR image.
D, Portal venous phase fat-suppressed T1-weighted MR image.

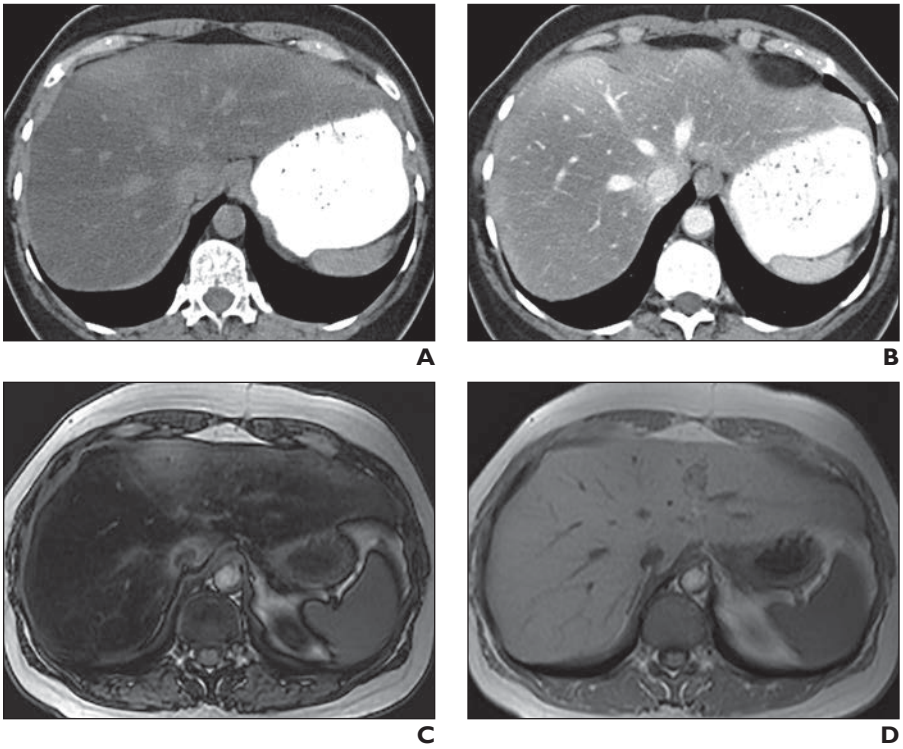

Fig. 11—29-year-old woman with abdominal pain. Example of diffuse fatty infiltration.
A, Unenhanced CT image shows diffuse decreased attenuation of hepatic parenchyma with areas of sheetlike fat sparing along capsule.
B, Contrast-enhanced CT image.
C, Out-of-phase T1-weighted MR image shows considerable loss of signal intensity compared with **D** and areas of fat sparing.
D, In-phase T1-weighted MR image.

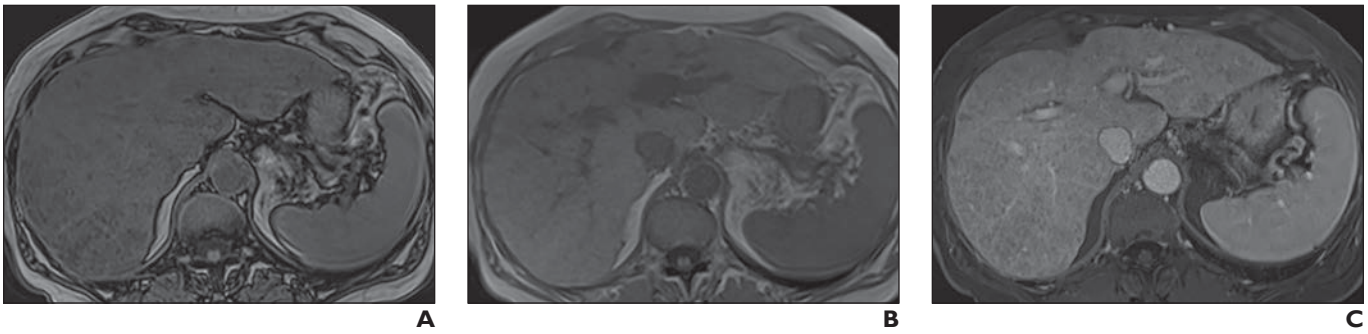

Fig. 12—70-year-old woman with nonalcoholic steatohepatitis and cirrhosis. Example of irregular nodular fatty infiltration. Occasionally, fatty change may have more diffuse nodular pattern, as in these images.
A, Out-of-phase T1-weighted MR image.
B, In-phase T1-weighted MR image.
C, Portal venous phase fat-suppressed T1-weighted MR image.

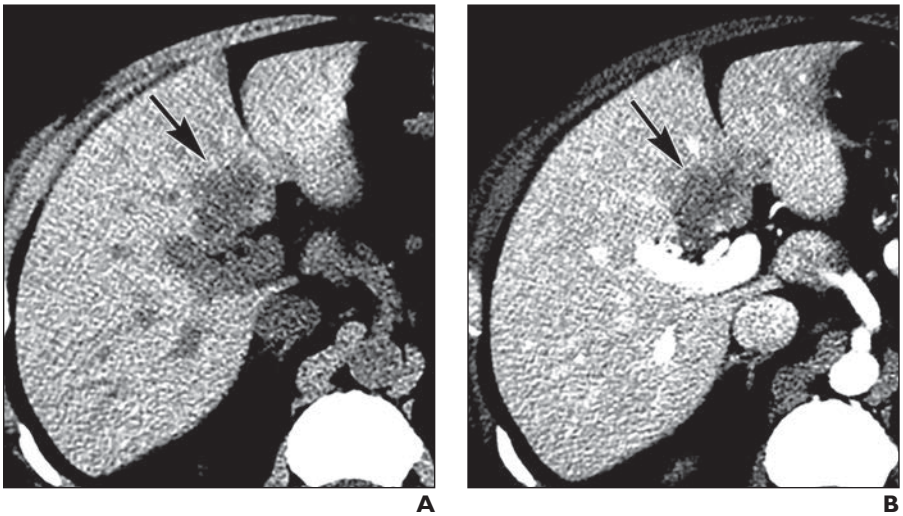

Fig. 13—51-year-old man with focal fatty infiltration.
A, Unenhanced CT image shows area of geographic lower attenuation (*arrow*) in segment IV of liver.
B, Portal venous phase CT image shows little change (*arrow*) over **A.**

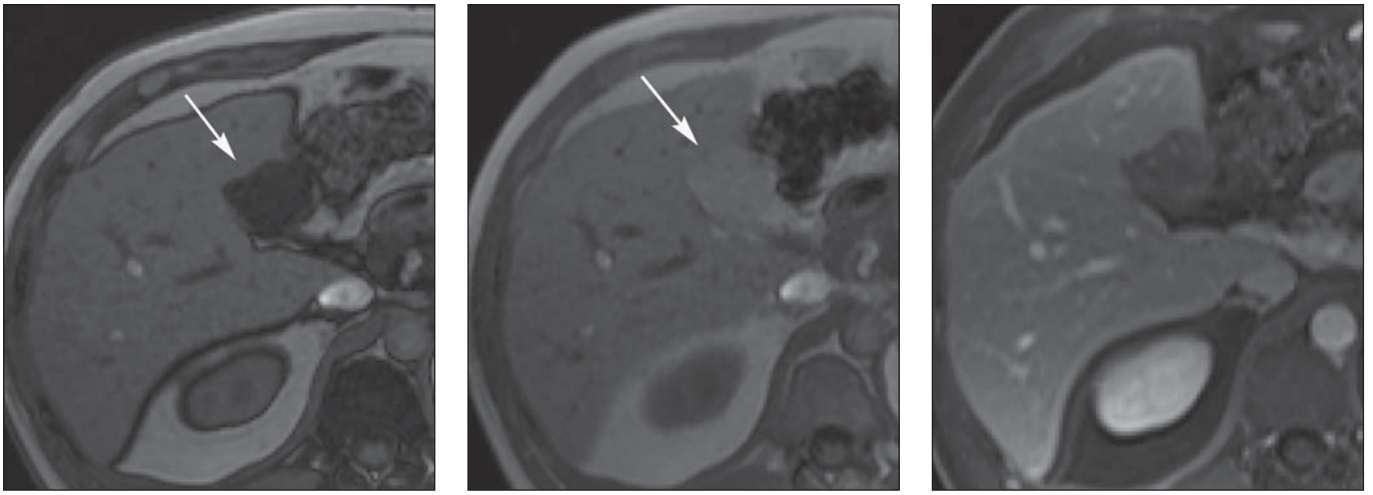

Fig. 14—45-year-old woman with hepatitis B. MRI observation is loss of signal intensity (*arrow*) on T1-weighted out-of-phase images compared with corresponding in-phase images, consistent with fat content. After IV contrast administration, observation is pattern of enhancement that is diminished in all phases (portal venous phase shown) without differential enhancement compared with background liver and thus simulates stamplike appearance of lower signal intensity with no change in size or signal intensity over various phases of contrast enhancement. This is typical of fatty infiltration.
A, Out-of-phase T1-weighted image.
B, In-phase T1-weighted image.
C, Portal venous phase fat-suppressed T1-weighted MR image.

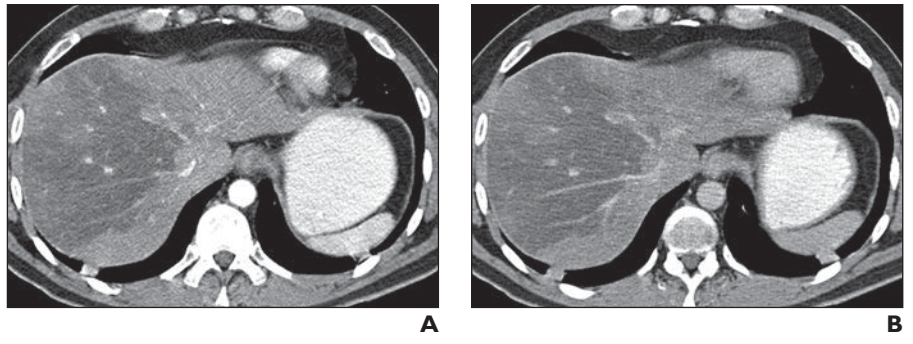

Fig. 15—46-year-old man with alcoholism. Example of geographic fatty infiltration. Well-defined areas of diminished attenuation in hepatic dome present in portal venous phase do not exhibit any overall change in delayed phase, typical of fatty infiltration. Vessels coursing through this region are not displaced. Both of these findings argue against presence of infiltrative mass and represent fatty infiltration.
A, Portal venous phase contrast-enhanced CT image.
B, Three-minute delayed phase contrast-enhanced CT image.

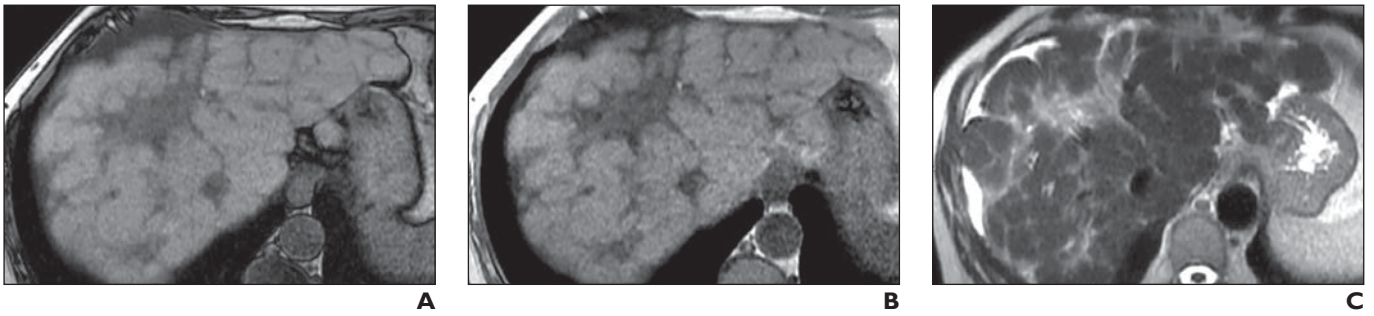

Fig. 16—55-year-old man with cirrhosis. Example of confluent fibrosis. MR images show sheetlike areas of increased signal intensity on T2-weighted image, decreased signal intensity on T1-weighted image, and delayed phase enhancement. This is typical of confluent fibrosis. Occasionally, areas of hyperenhancement may be present on arterial phase images. Areas of capsular retraction and volume loss may accompany fibrosis.
A, Out-of-phase T1-weighted MR image.
B, In-phase T1-weighted MR image.
C, T2-weighted MR image.

(Fig. 3 continues on next page)

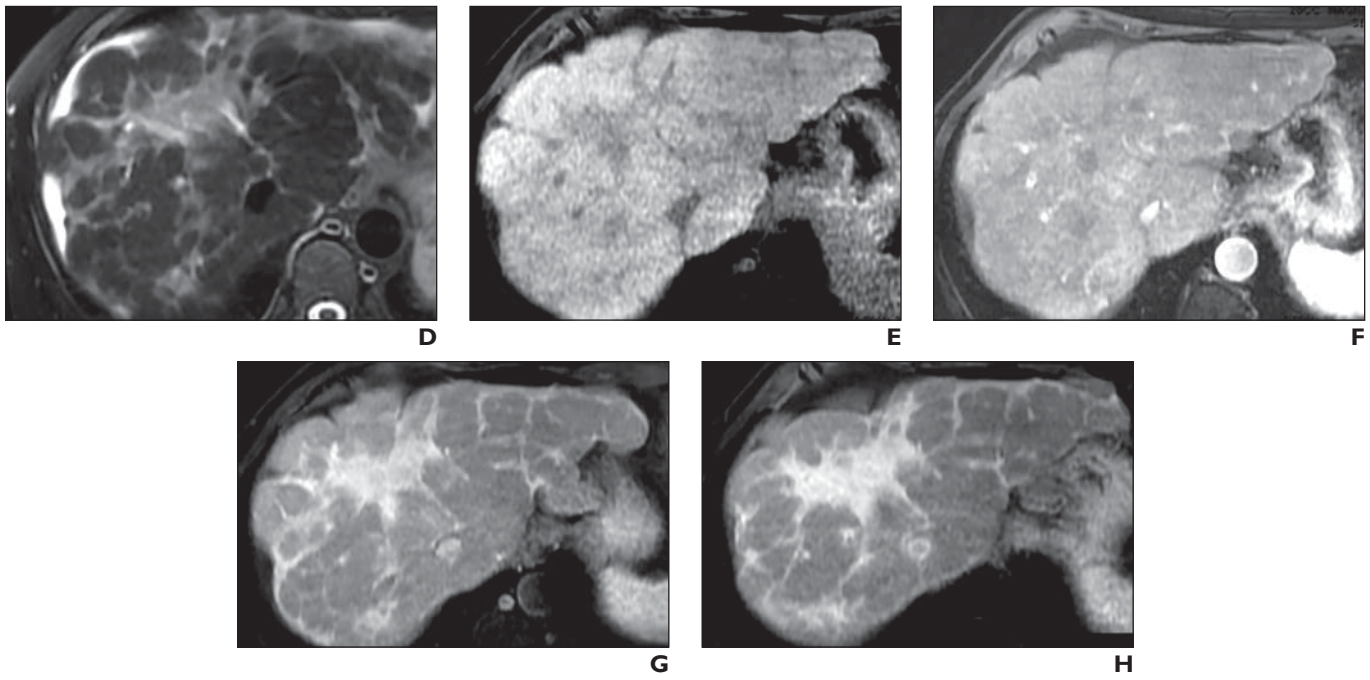

Fig. 16 (continued)—55-year-old man with cirrhosis. Example of confluent fibrosis. MR images show sheetlike areas of increased signal intensity on T2-weighted image, decreased signal intensity on T1-weighted image, and delayed phase enhancement. This is typical of confluent fibrosis. Occasionally, areas of hyperenhancement may be present on arterial phase images. Areas of capsular retraction and volume loss may accompany fibrosis.
D, Fat-suppressed T2-weighted MR image.
E, Unenhanced fat-suppressed T1-weighted MR image.
F, Arterial phase fat-suppressed T1-weighted MR image.
G, Portal venous phase fat-suppressed T1-weighted MR image.
H, Five-minute delayed venous phase fat-suppressed T1-weighted MR image.

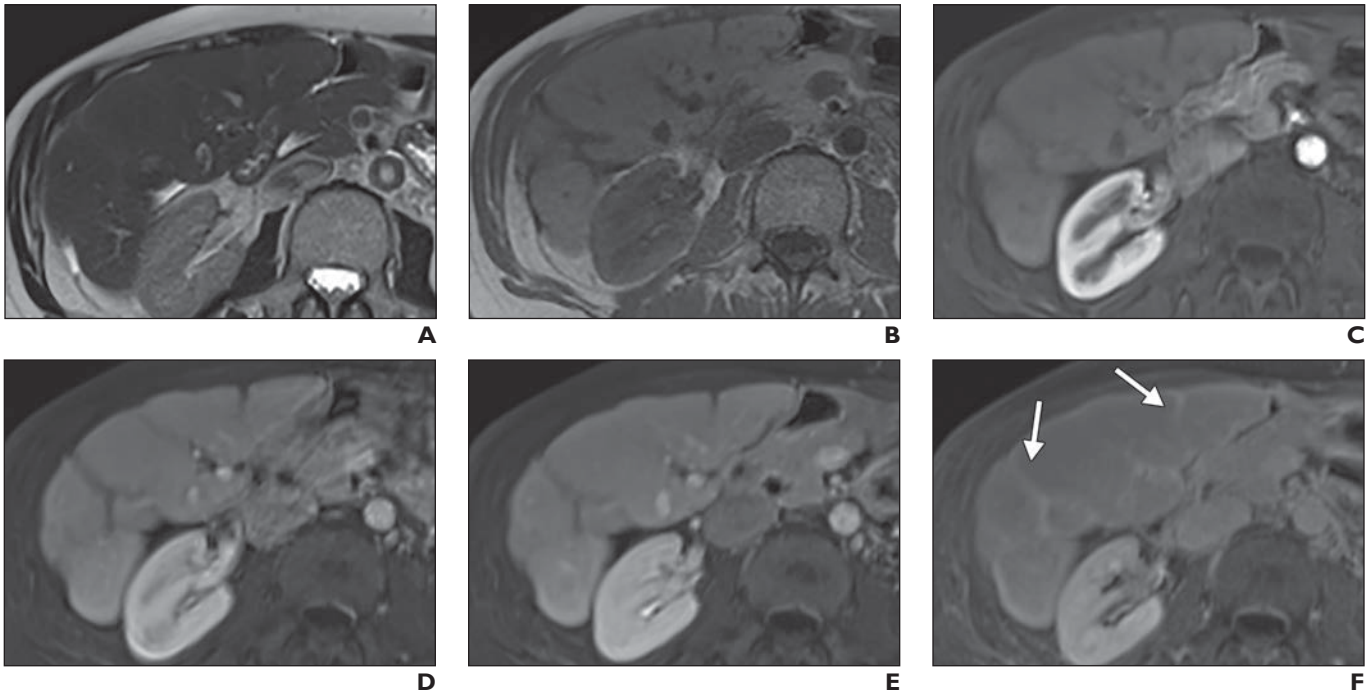

Fig. 17—48-year-old woman with cirrhosis for 12 years. Example of focal scar. Bandlike areas of increased signal intensity are present on T2-weighted and decreased signal intensity on T1-weighted image with delayed phase enhancement (*arrows,* **F**). This is typical of focal scar and fibrosis. Areas of capsular retraction and volume loss accompany this finding.
A, T2-weighted MR image.
B, T1-weighted MR image.
C, Arterial phase fat-suppressed T1-weighted MR image.
D, Portal venous phase fat-suppressed T1-weighted MR image.
E, Three-minute delayed venous phase fat-suppressed T1-weighted image.
F, Five-minute delayed venous phase fat-suppressed T1-weighted image.

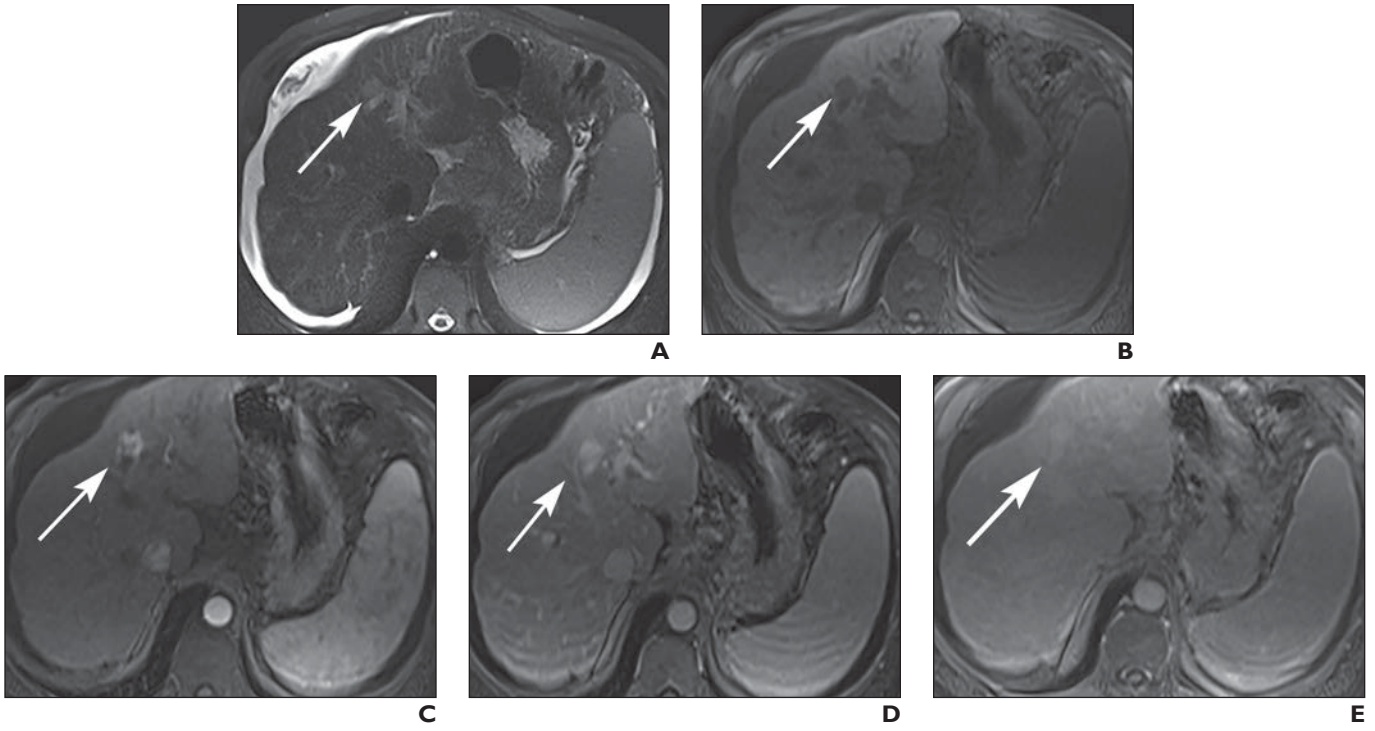

Fig. 18—65-year-old man with cirrhosis and cholangiocarcinoma. Observations are vague small area (*arrow,* **A** and **B**) of increased signal intensity on T2-weighted image, decreased signal intensity on T1-weighted image, arterial phase hyperenhancement, and progressive hyperintensity on later phase images. Biopsy was performed because of features worrisome for cholangiocarcinoma.
A, Fat-suppressed T2-weighted MR image.
B, Unenhanced fat-suppressed T1-weighted image.
C, Arterial phase fat-suppressed T1-weighted MR image.
D, Portal venous phase fat-suppressed T1-weighted MR image.
E, Five-minute delayed venous phase fat-suppressed T1-weighted image.

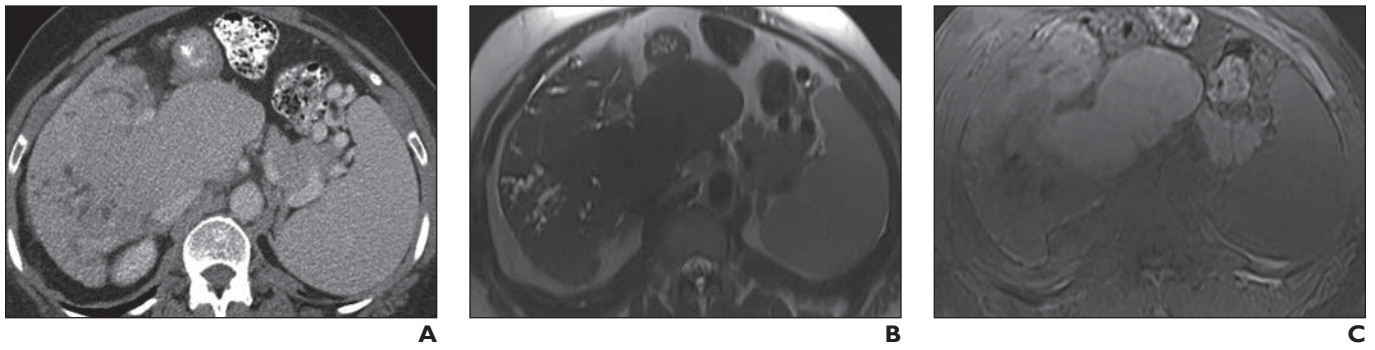

Fig. 19—65-year-old woman with primary sclerosing cholangitis. Example of hypertrophic pseudomass. Cirrhotic liver may have regions of atrophic and hypertrophic change. Areas of hypertrophy may appear masslike, especially if localized to portion of liver. Certain disease processes are associated with marked central hypertrophy, as in sclerosing cholangitis, chronic Budd-Chiari syndrome, and chronic portal venous obstruction. Marked enlargement of caudate lobe with irregular mildly dilated bile ducts is evident closer to periphery.
A, IV contrast-enhanced CT image.
B, T2-weighted MR image shows areas of regenerative hypertrophy as areas of low signal intensity compared with more fibrotic atrophic portions of liver, which have higher signal intensity.
C, Fat-suppressed T1-weighted MR image shows areas of regenerative hypertrophy have high signal intensity compared with more fibrotic atrophic portions of liver, which have low signal intensity.

(Fig. 19 continues on next page)

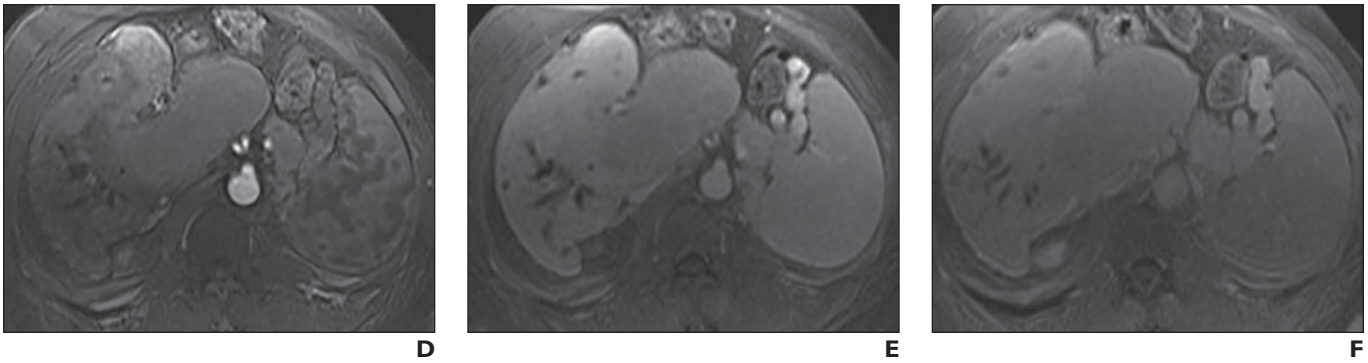

Fig. 19 (continued)—65-year-old woman with primary sclerosing cholangitis. Example of hypertrophic pseudomass. Cirrhotic liver may have regions of atrophic and hypertrophic change. Areas of hypertrophy may appear masslike, especially if localized to portion of liver. Certain disease processes are associated with marked central hypertrophy, as in sclerosing cholangitis, chronic Budd-Chiari syndrome, and chronic portal venous obstruction. Marked enlargement of caudate lobe with irregular mildly dilated bile ducts is evident closer to periphery.
D, Arterial phase fat-suppressed T1-weighted MR image shows high and low signal-intensity pattern similar to that in **C.**
E, Portal venous phase fat-suppressed T1-weighted MR image shows high- and low-signal-intensity pattern similar to that in **C.**
F, Three-minute delayed venous phase fat-suppressed T1-weighted image. Regenerative regions often appear as masslike areas of hypointensity on delayed contrast-enhanced images compared with peripheral portions of liver that exhibit delayed phase enhancement typical of fibrosis.

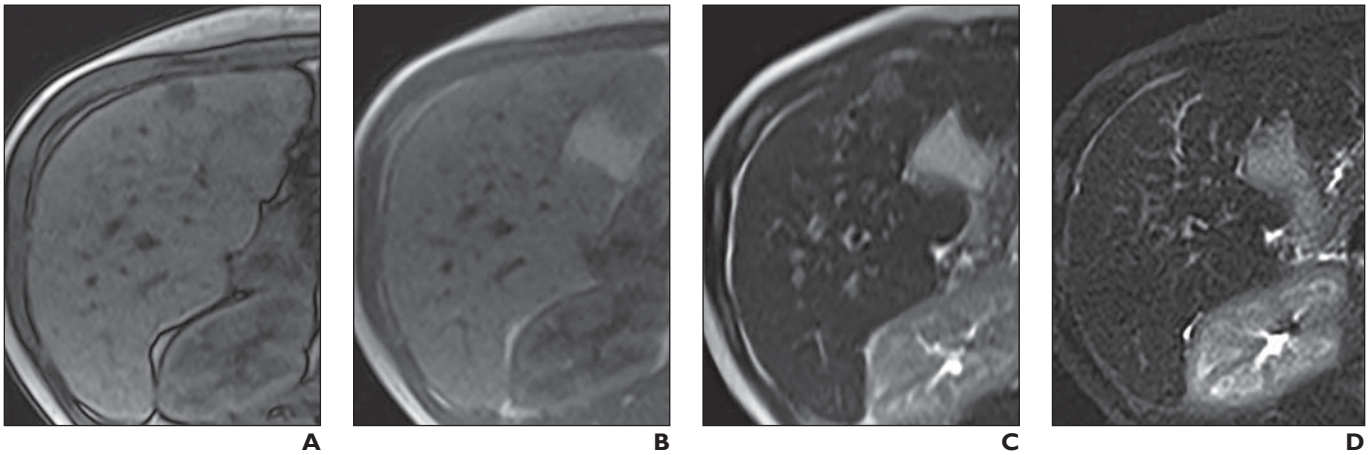

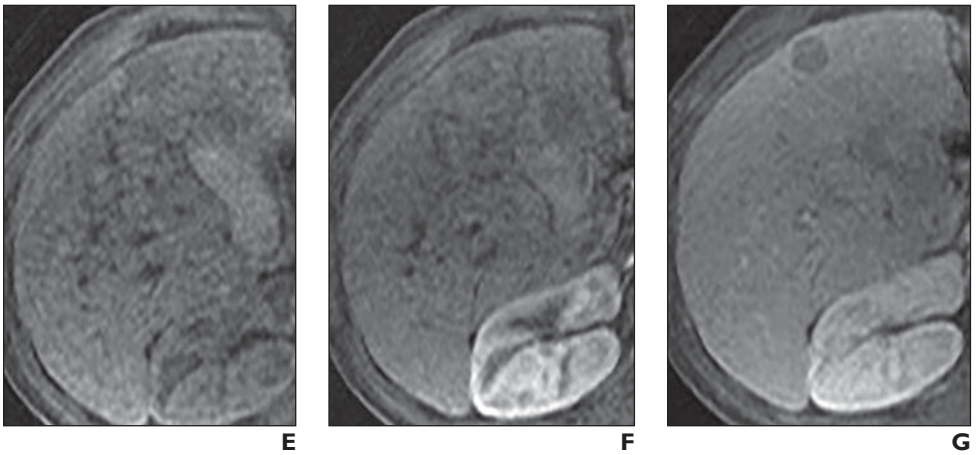

Fig. 20—8-year-old boy with benign steatotic nodules. Small nodule exhibits loss of signal intensity on T1-weighted out-of-phase MR images compared with in-phase images. Lesion has increased signal intensity on T2-weighted single-shot fast spin-echo images but is isointense in relation to liver on T2-weighted fat-suppressed images. No hyperenhancing components are present, and lesion remains of diminished signal intensity in all phases after contrast injection. These nodules were stable on follow-up examination 5 years later.
A, Out-of-phase T1-weighted MR image.
B, In-phase T1-weighted MR image.
C, T2-weighted MR image.
D, Fat-suppressed T2-weighted MR image.
E, Unenhanced fat-suppressed T1-weighted image.
F, Arterial phase fat-suppressed T1-weighted MR image.
G, Three-minute delayed venous phase fat-suppressed T1-weighted image.

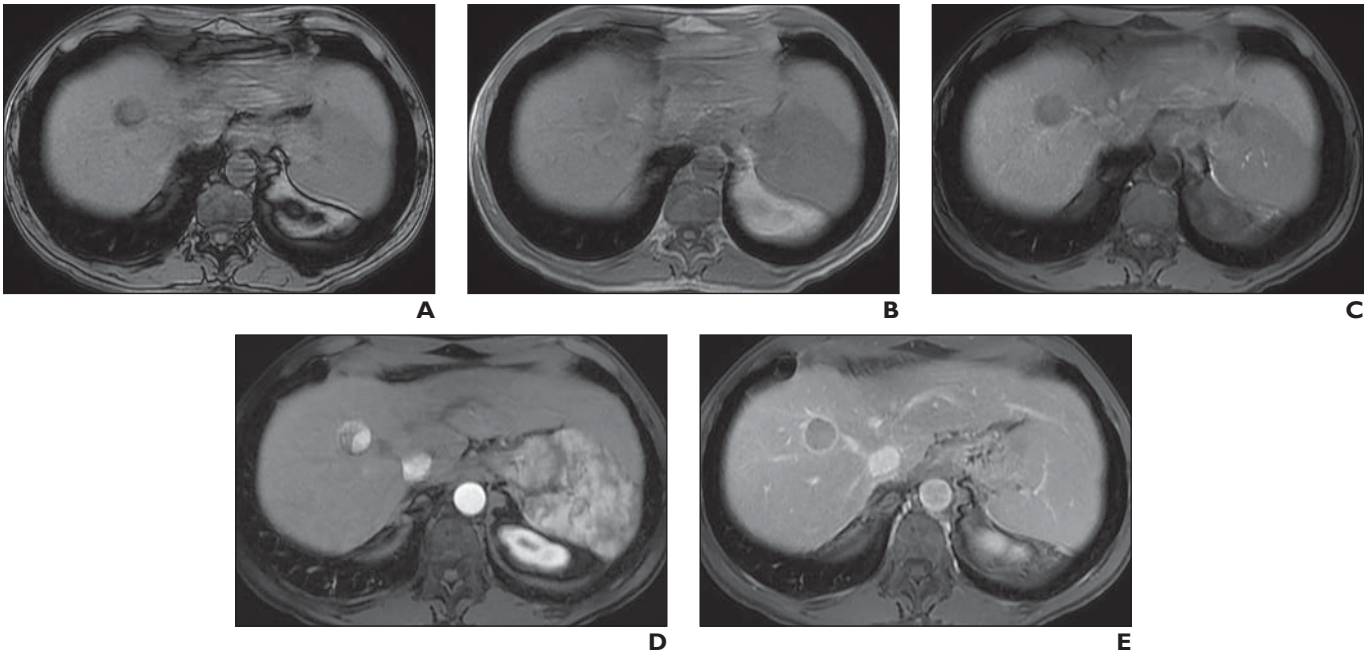

Fig. 21—63-year-old man with hepatitis C and hepatocellular carcinoma. Example of intralesional steatosis. Lesion exhibits loss of signal intensity on out-of-phase T1-weighted MR images compared with in-phase images. Lesion has increased signal intensity on T2-weighted single-shot fast spin-echo and T2-weighted fat-suppressed images. Lesion measures 2.1 cm and exhibits arterial phase enhancement compared with unenhanced images and washout on later phase images with capsule present; therefore it is assigned to LI-RADS category 5.
A, Out-of-phase T1-weighted MR image.
B, In-phase T1-weighted MR image.
C, Unenhanced fat-suppressed T1-weighted MR image.
D, Arterial phase fat-suppressed T1-weighted MR image.
E, Three-minute delayed venous phase fat-suppressed T1-weighted image.

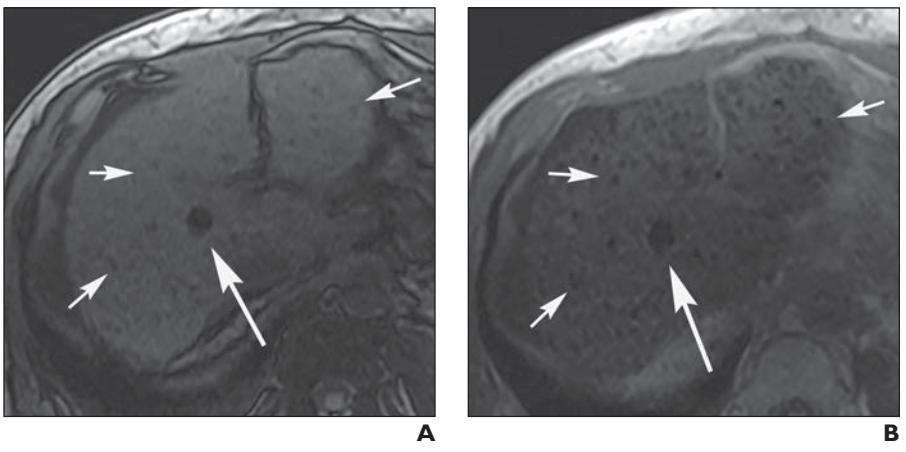

Fig. 22—51-year-old man with hepatitis C and siderotic nodules. Multiple tiny areas of diminished signal intensity (*short arrows*) on T1-weighted out-of-phase images exhibit loss of signal intensity or blooming artifact on in-phase images with longer TE. This is typical appearance of siderotic nodules, which are highly visible on T1-weighted fat-suppressed gradient recalled-echo images. Transjugular intrahepatic portosystemic shunt catheter is present with associated blooming artifact (*long arrow*).
A, Out-of-phase T1-weighted MR image (TE, 2.3 ms).
B, In-phase T1-weighted MR image (TE, 4.5 ms).

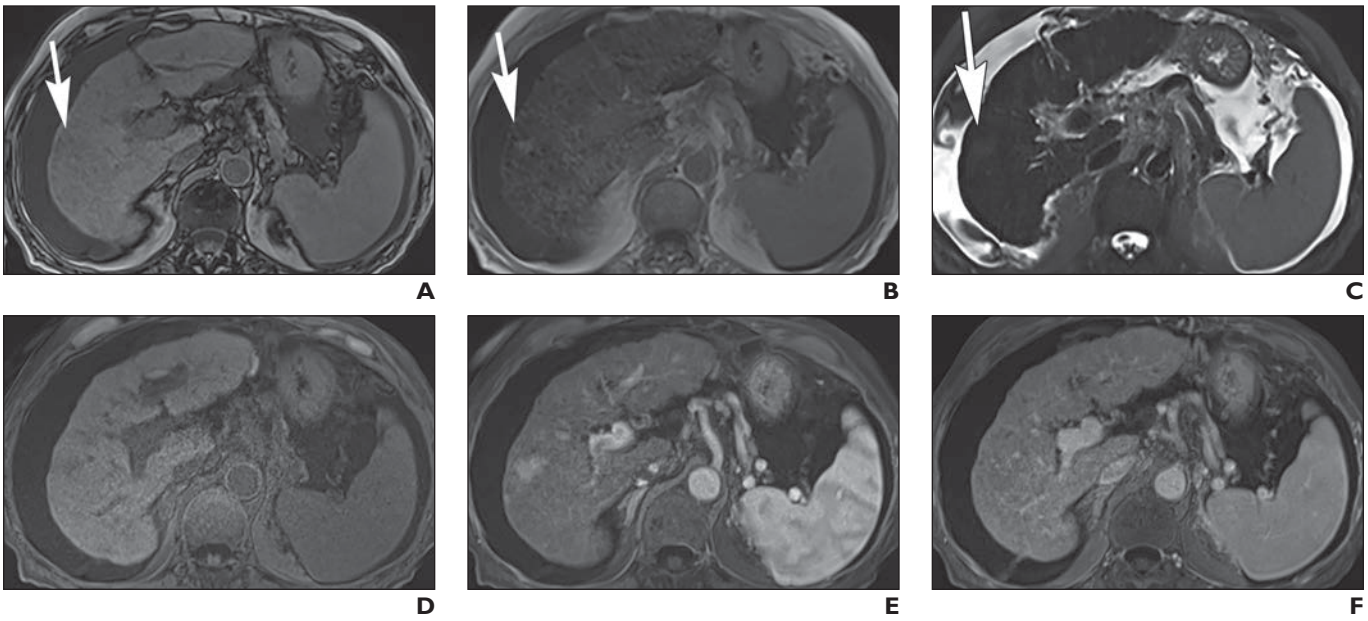

Fig. 23—77-year-old woman with hepatitis C cirrhosis with iron-sparing in region of liver mass. Nodular and diffuse areas of loss of signal intensity are present throughout cirrhotic liver on in-phase T1-weighted MR images with longer TE compared with corresponding out-of-phase images, consistent with susceptibility artifact induced by iron deposition. Small (1.7-cm) area of iron sparing (*arrow,* **A**–**C**) is evident in right hepatic lobe with mildly increased signal intensity on arterial phase T2-weighted image. Assignment was LI-RADS category 3.
A, Out-of-phase T1-weighted MR image.
B, In-phase T1-weighted MR image.
C, Fat-suppressed T2-weighted MR image.
D, Unenhanced fat-suppressed T1-weighted image.
E, Arterial phase fat-suppressed T1-weighted MR image
F, Portal venous phase fat-suppressed T1-weighted MR image.

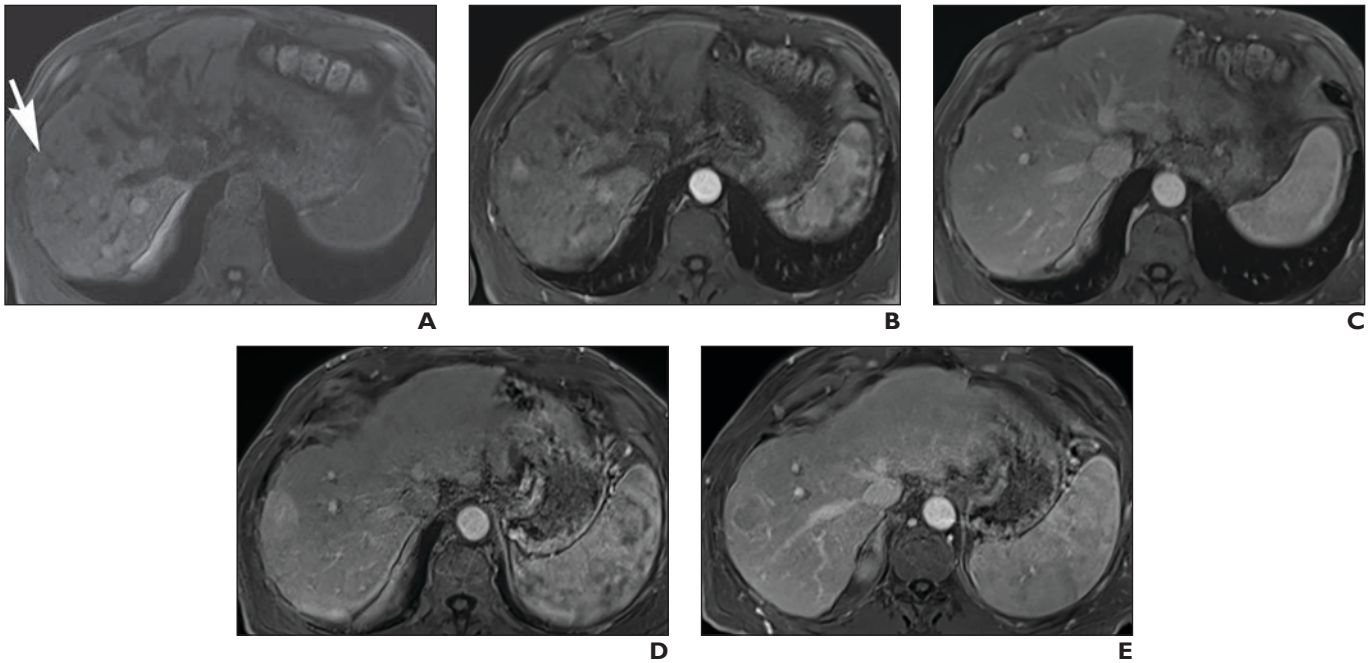

Fig. 24—62-year-old man with alcoholic cirrhosis and hepatocellular carcinoma (HCC). Example of distinctive nodule that develops into HCC. Initial MR images of atypical nodules (*arrow,* **A**) show increased signal intensity on T1-weighted images and isointensity on T2-weighted images (not shown) with questionable enhancement on early arterial phase images (**A**–**C**) without washout. Four months later (**D** and **E**), lesion in subcapsular portion of segment VIII exhibits arterial phase enhancement and washout and measures larger than 2 cm.
A, Initial unenhanced fat-suppressed T1-weighted image.
B, Initial arterial phase fat-suppressed T1-weighted MR image
C, Initial portal venous phase fat-suppressed T1-weighted MR image.
D, Arterial phase T1-weighted fat-suppressed image obtained 4 months after **A**–**C.**
E, Portal venous phase fat-suppressed T1-weighted MR image obtained 4 months after **A**–**C.**

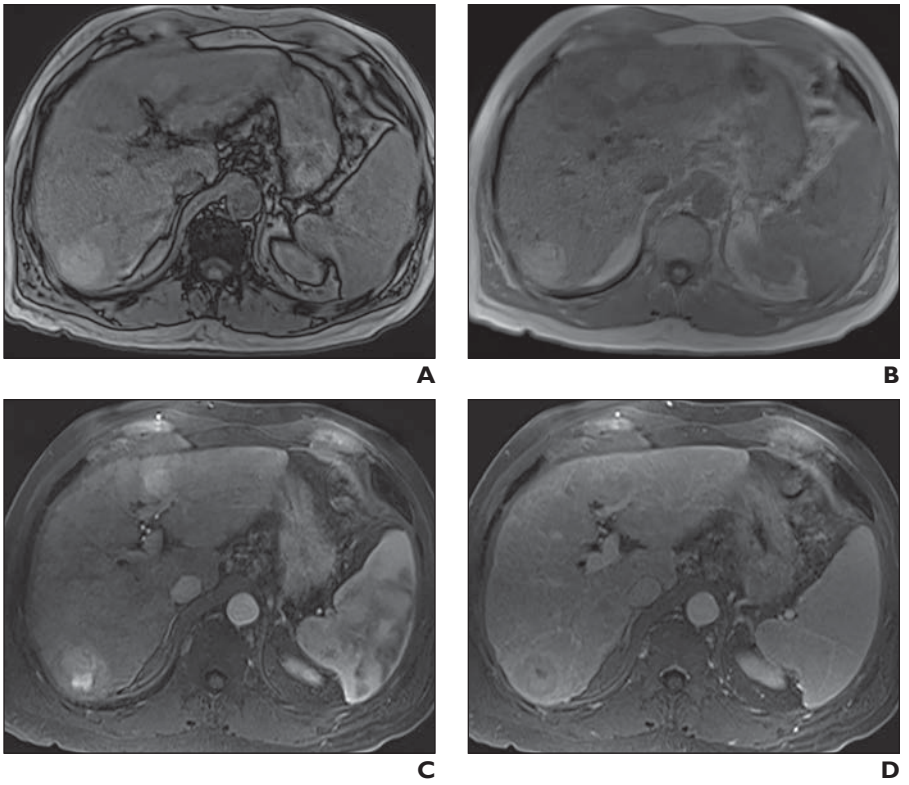

Fig. 25—64-year-old man with hepatitis C cirrhosis and biopsy-proven hepatocellular carcinoma (HCC) with increased signal intensity on T1-weighted MR images. Segment VII lesion had increased signal intensity on unenhanced T1-weighted image (**A**). Comparison of T1-weighted out-of-phase (**A**) and in-phase (**B**) images shows no evidence of intralesional steatosis. Lesion had heterogeneous signal intensity on T2-weighted images (not shown). There is heterogeneous arterial phase enhancement with washout (**C** and **D**). Biopsy was performed at outside institution with pathologic confirmation of HCC. Several additional lesions consistent with LI-RADS category 5 excluded patient from undergoing liver transplantation.
A, Out-of-phase T1-weighted MR image.
B, In-phase T1-weighted MR image.
C, Arterial phase fat-suppressed T1-weighted MR image.
D, Portal venous phase fat-suppressed T1-weighted MR image.

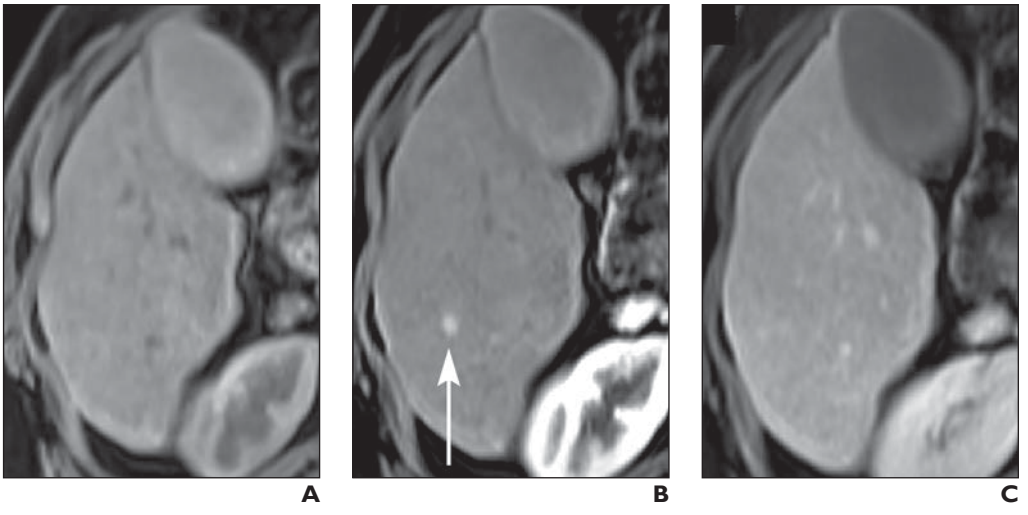

Fig. 26—51-year-old man with hepatitis C. Typical nodulelike area of hyperenhancement (NAPH) is present on arterial phase images and was invisible in other later phases. No corresponding signal-intensity abnormalities are present on unenhanced T1-weighted image.
A, Unenhanced fat-suppressed T1-weighted MR image.
B, Arterial phase fat-suppressed T1-weighted MR image.
C, Portal venous phases fat-suppressed T1-weighted MR image.

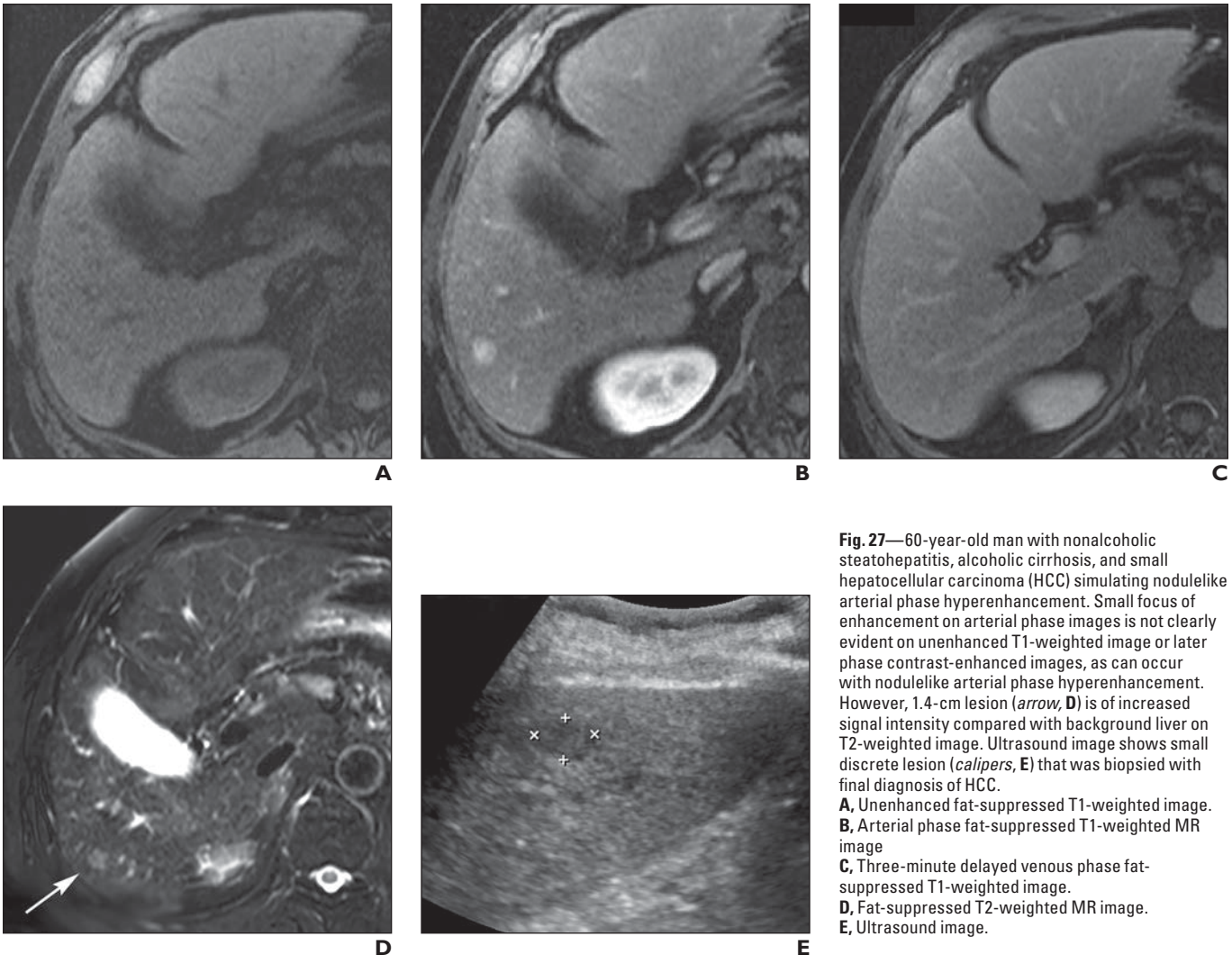

Fig. 27—60-year-old man with nonalcoholic steatohepatitis, alcoholic cirrhosis, and small hepatocellular carcinoma (HCC) simulating nodulelike arterial phase hyperenhancement. Small focus of enhancement on arterial phase images is not clearly evident on unenhanced T1-weighted image or later phase contrast-enhanced images, as can occur with nodulelike arterial phase hyperenhancement. However, 1.4-cm lesion (*arrow*, **D**) is of increased signal intensity compared with background liver on T2-weighted image. Ultrasound image shows small discrete lesion (*calipers*, **E**) that was biopsied with final diagnosis of HCC.
A, Unenhanced fat-suppressed T1-weighted image.
B, Arterial phase fat-suppressed T1-weighted MR image
C, Three-minute delayed venous phase fat-suppressed T1-weighted image.
D, Fat-suppressed T2-weighted MR image.
E, Ultrasound image.